Interfacial Thermal Resistance Measurements of Solution Deposited CNT Films on Copper Substrates

by

Yi Zheng

A thesis submitted to the Graduate Faculty of
Auburn University
in partial fulfillment of the
requirements for the Degree of
Master of Science

Auburn, Alabama
August 1, 2015

Keywords: thermal resistance, CNTs, TIM tester

Approved by

Daniel K. Harris, Chair, Associate Professor of Mechanical Engineering
Michael C. Hamilton, Assistant Professor of Electrical and Computer Engineering
Daniel Mackowski, Professor of Mechanical Engineering

Abstract

Carbon nanotubes (CNTs) have been regarded as one of the most promising materials for electronics applications during the past two decades according to their outstanding electrical properties. However, the fabrication method of CNTs is an important matter since the materials need to be managed easily as well as placed precisely when being applied in electronics. Xu and Hamilton [1] - [2] found an effective solution based application method which can meet those requirements while the process is done at room temperature. This is better than some of the most commonly found methods, such as chemical vapor deposition (CVD), which needs high fabrication temperatures. High fabrication temperatures can cause deformation due to any coefficient of thermal expansion (CTE) mismatches. Their groundbreaking work showed that the electrical properties of CNTs didn't have a large influence during the fabrication process through both experiment and modeling. However, the thermal interfacial behavior of solution deposited CNT films needed to be characterized.

In this thesis, the interfacial thermal impedance of the CNTs, which were fabricated by the method of Xu and Hamilton [1] - [2] was studied. A TIM Tester Model 1400 using ASTM D5470 method by Analysis Tech Inc. was used to characterize the thermal resistance of inkjet CNT films. Copper Alloy 110 disks were used as fabrication substrates on which the ink was printed. The volumes of CNT dispersion were controlled for 2 mL, 4mL, 6 mL and 8 mL. Two groups of samples which were single sided and double sided were tested under four different pressures: 20 psi, 40 psi, 60 psi and 80 psi. Every single test was repeated for 10 times in order to

obtain reliable data. The average heat resistances of the last five tests are shown in Table 3.10. All data is listed in appendix. A group of bare copper substrates without MWNTs films was also tested under same conditions as a control reference. The results show a heat insulating, electrical conducting CNTs film using this kind of solution-based application method was obtained.

Acknowledgments

This thesis is the last step of obtaining my Master of Science degree in the Department of Mechanical Engineering at Auburn University. After studying at Auburn University for three years, I have many people I would like to thank. I would not have been able to complete my thesis and gained my degree without their help.

First, I would like to express my special thanks and gratitude to my advisor, Dr. Daniel K. Harris for his support of my study and research. He uses patience, motivation, enthusiasm and immense knowledge to guide me in all the time spent doing my research and writing my thesis. His experience and knowledge always helped me when I faced difficulties. His trust in me made me feel confident to deal with all obstacles.

Next, I would like to thank Dr. Michael Hamilton and his student, Dr. Pingye Xu in the Department of Electrical and Computer Engineering. Dr. Michael Hamilton guided and taught me a lot about electrical engineering during our meetings. He also gave me many useful pieces of advice as my thesis committee member. Dr. Pingye Xu helped me solve the problems about the carbon nanotube in fabrication and electrical transport.

Thirdly, I want to thank Dr. Daniel Mackowski in the Department of Mechanical Engineering for serving as a committee member and for his encouragement, insightful comments, and hard questions. His course “Conduction & Radiation Heat Transfer” really interested me and helped me a lot during my research.

I am also grateful to Mr. Roy Chandon, a Ph.D. candidate in my research group. Whenever I faced problems with testing and writing, he always advised and instructed me a lot.

I would also like to thank all my friends here in Auburn. I am thankful for them for accompanying and supporting me when I was away from my family and my friends back home.

Additionally, I am so grateful to my family for supporting me while I studied abroad at Auburn University. They always supported me to do anything. I am missing them so much.

Finally, I would like to express my appreciation to the Department of Mechanical Engineering at Auburn University by supporting and funding my study through a teaching assistantship position.

Table of Contents

List of Tables

List of Figures

List of Abbreviations

CNTs	Carbon Nanotubes
CVD	Chemical Vapor Deposition
CTE	Coefficient of Thermal Expansion
MWNTs	Multi-walled Carbon Nanotubes
SWNTs	Single-walled Carbon Nanotubes
FIT	Fluctuation-induced Tunneling
Pt	Platinum
EB	Electron Beam
PPR	Pulsed Photothermal Reflection
TIMs	Thermal Interface Materials
PCMs	Phase Change Materials
PSTTR	Phase Sensitive Transient Thermos-Reflectance
EPD	Electrophoretic Deposition
SDS	Sodium Dodecyl Sulfate
DI	Deionized

Chapter 1

Introduction

Carbon Nanotubes (CNTs) are the most popular research members in the Buckminsterfullerenes families since their first observation in 1991, which was credited to Lijima [3]. CNTs are cylindrical nanostructures, whose maximum length can be up to 18.5 cm, while their widths are around 1 nm [4]. This means the length is one hundred million times larger than the width, which is significantly different than other materials. Normally, CNTs are divided into two main categories: single-walled carbon nanotubes (SWNTs) and multi-walled carbon nanotubes (MWNTs).

Extensive research and studies about the CNTs have been done in the last twenty years and will continue because of their increasing potential applications due to their outstanding electrical properties. [5] However, the fabrication method of CNTs is one of the important problems that can limit the application of CNTs in electronics. This is because how to place CNTs precisely and manipulating them easily is still challenging [6]. The most effective and common fabrication method nowadays is chemical vapor deposition (CVD) which can meet those challenges well, but there is one shortcoming of this kind of method which is a high processing temperature. The high processing temperature may cause the coefficient of thermal expansion (CTE) mismatch as well as influence the electrical and mechanical properties. The coefficient of thermal expansion (CTE) is one of the parameters which can characterize the thermal properties of the material by calculating the ratio of the degree of expansion to the temperature difference and the mismatch of CTE may cause deformation and lead to failed production.

Xu et al. found a solution-based fabrication method of CNTs which can deal with those challenges successfully under the room temperature to avoid the effects by high processing temperature. Otherwise, the electrical properties were proved without a large influence during the fabrication process by both experiments and fluctuation-induced tunneling (FIT) model [1].

However, the thermal properties of Xu's solution deposited CNT films are needed to be further characterized. As a solid material, the thermal conductivity of the CNTs is the most important research field about the thermal properties. The highest theoretical thermal conductivity of CNTs can go up to 37,000 W/mK [7], while another study got a value of 200W/mK [8]. And a result of 0.13-0.20 W/mK of thermal conductivity of CNTs was also be obtained by Prasher et al [9]. Multiple researches show different results according to various conditions.

There are lots of factors that can influence the thermal conductivity of the materials, the most significant one being interfacial thermal resistance. So, in this thesis, the interfacial thermal resistance measurements of solution deposited CNT films fabricated by Xu's method are determined.

Chapter 2

Literature Review

2.1: CNTS

Carbon has been used by the human being for a long time since ancient ages by its miscellaneous forms [10]. The history of CNTs is just several decades. In general, we agree that Sumio Lijima, working in the fundamental research laboratories for NEC Corporation, was credited to be the first person of discovering CNTs in 1991. In his Nature paper, he reported a new structure of carbon that is a needle like tube. Those needles were produced by using an arc-discharge evaporation and grew at the negative side of the electrode. He also found that every needle contained 2 - 50 coaxial tubes of graphitic sheets, and the hexagons of the carbon atom were helical which were different from each tube as well as needles by electron microscopy. He suggested that more research about the carbon structures on scales could be considered [3]. After this paper, more and more researchers were inspired and got involved in the carbon nanotube field.

Although the history of CNTs is not very long, lots of tremendous contributions were made in this area. The thermal proporties of CNTs are one of the most attractive and important study field of the CNTs researches. According to the vast amounts of literature, CNTs were reported to show outstanding mechanical, electrical and thermal properties.

Rodney and Donald predicted the thermal properties of CNTs from graphite whose properties are well known. They felt that the on-axis thermal conductivity of CNTs was possibly larger than that of diamond while the radial thermal conductivity of MWNTs might be lower than that of c-axis graphite. A high on-axis thermal conductivity of the carbon fibers was obtained by experiment since the calculation cannot be done easily. a conclusion of isotropic was expected about the thermal coefficient of expansion of the ideal CNTs, including SWNTs and MWNTs [11].

Much more studies had been done on the thermal properties of CNTs after those predictions. Since MWNTs are the materials we used in this thesis, more literature about thermal properties of MWNTs was reviewed.

Kim et al. used a microfabricated suspended device with a single MWNTs hybridized to measure the thermal performance in 2001. Figure 2.1 shows the representative fabricated microdevice. Two 10 μm ×10 μm islands with 0.5 μm thick silicon nitride membrane and 200 μm long silicon nitride beams were suspended by three 250 μm silicon nitrides legs. Thin platinum (Pt) film resistors fabricated by electron beam lithography were electrically connected by the Pt lines on the legs as a heater to connect the microthermometer and the bonding pads. Then the MWNTs were placed on the designated part of the microdevice by mechanical manipulation to bridge two islands. The diameter of the tested single MWNT was 14 nm while the length of the bridging segment was 2.5 μm. The thermal conductivity of the junction between the tested individual MWNT and the island was neglected. A result of 3000 W/K was obtained for the thermal conductivity of the individual MWNT at room temperature, which was two orders of magnitude higher than that of macroscopic mat samples. The phonon mean free path was obtained to be about 500nm. Due to the onset of umklapp phonon scattering, a peak at 320 K was showed for the temperature dependence of the thermal conductivity of the MWNTs [12].

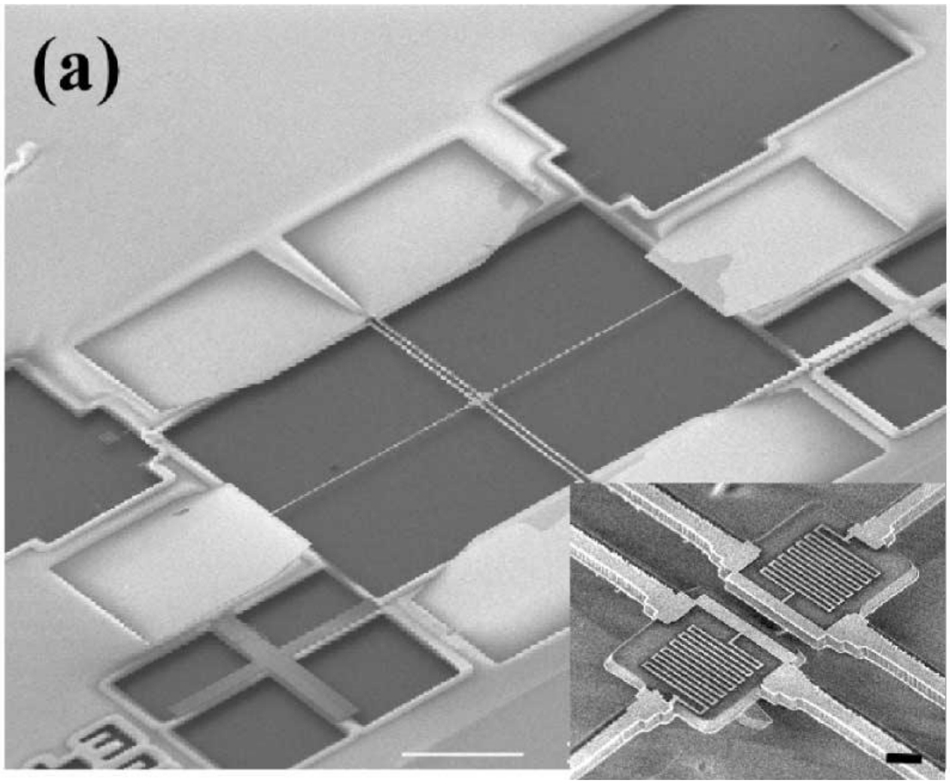

Figure 2.1 A Large Scale Scanning Electron Microscopy (SEM) Image of a Microfabricated Device Inset: Enlarged Image of the Suspended Islands with the Pt Resistors [12]

Choi et al. used a self-heating 3w method to measure the thermal conductivity of individual multiwalled carbon nanotubes in 2005. A result of 650 and 830 W/mK for the thermal conductivity of the two samples was found with a ±6% measurement error by placing an individual MWNT across the desired metal electrodes, followed with depositing Pt at the nanotube-metal contacts by electron-beam (EB) and then annealed the sample. The size of the MWNTs might be the reason for the difference in thermal conductivity of the two samples [13].

Yang et al. used a pulsed photothermal reflectance (PPR) technique to study the thermal conductivity of multiwalled carbon nanotubes film with the assumption of one dimensional heat conduction and heat loss neglect. Figure 2.2 shows the fabrication process of the test configuration. First, a high resistivity silicon wafer was prepared as a substrate. Second, a groove on the substrate with 10-50 μm depth and 3-5 mm width was ethced. Third, a 0.5-100 nm nickel film in the slot that was used to grow MWNTs in CH_4+H_2+N_2 microwave plasma as the catalyst was deposited. Fourth, the unwanted nickel was removed. Fifth, MWNTs with 200:20:10 for the ratio of H_2: CH_4: N_2 under temperature of 720 ℃ was grown with microwave power of 1300 W and deposition pressure of 35 Torr for 10 minutes. Last step was to attach a 1.2 μm thick gold foil on top of the sample [14].

Figure 2.3 shows a setup of the pulsed photothermal reflectance technique Yang et al. used to measure the thermal conductivity of MWNTs films. The sample was struck by the Pump Nd:YAG laser pulse with a pulse width of 8ns, a spot size of 3 mm, a pulse energy of 30.3 μJ and the frequency was 10 Hz [14].

A three layer heat conduction model was applied to determine the thermal conductivity of MWNTs films concerning the substrate as an infinite medium. The contact thermal resistance of foil-MWNTs was negligible since it did not have much influence on the thermal conductivity of MWNTs films while the heat loss could also be neglected due to the short measurement time of 400 μs. The measured results are summarized in Table 2.1. The average thermal conductivity of MWNTs films was obtained to be 15 W/mK. According to the data reported, the thermal conductivity of MWNTs was independent of the MWNTs length. The effective thermal conductivity could go up to 200 W/K if considering the volume filling fraction of the carbon nanotubes [14].

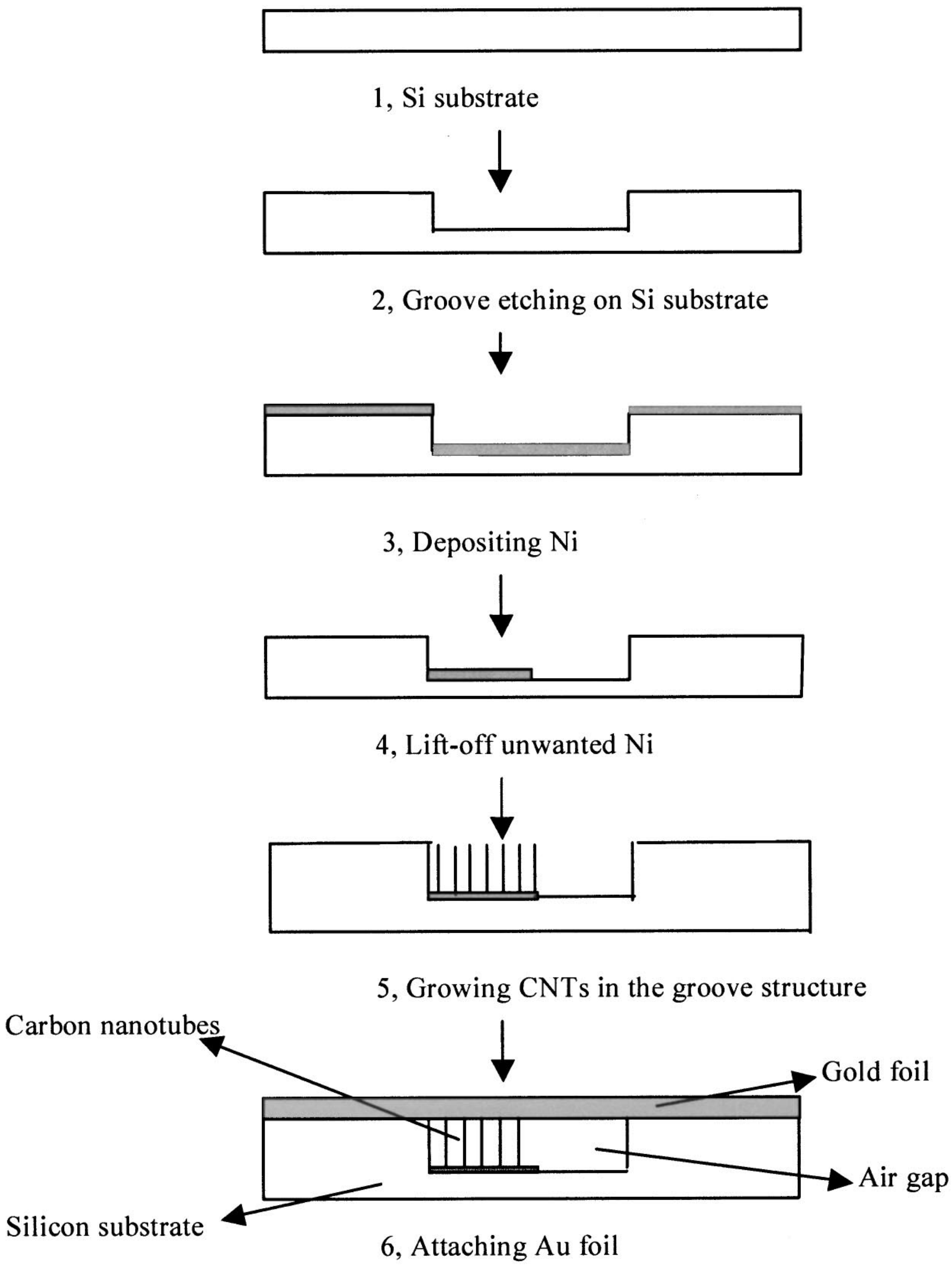

Figure 2.2 Procedures of the CNT Samples Preparation [14]

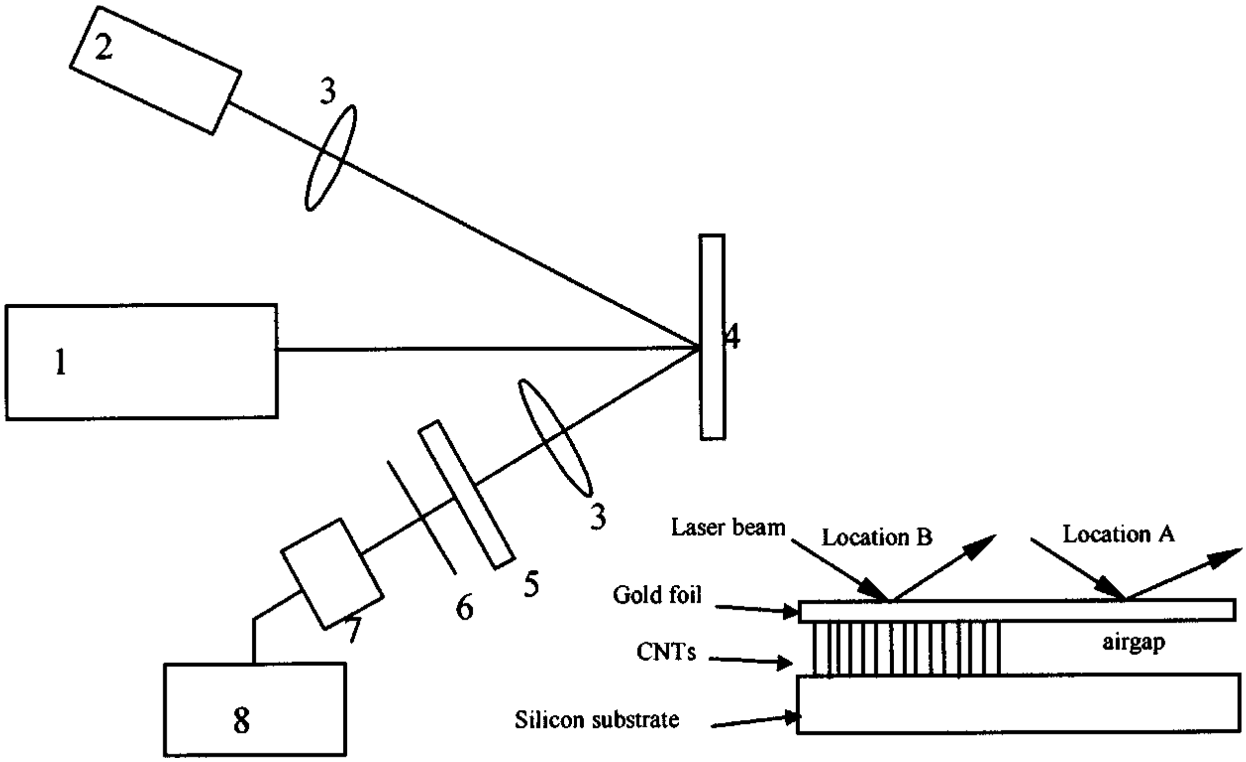

Figure 2.3 Photothermal Reflection Experiment Setup

(1) Pump Nd: YAG laser, (2) Probe He-Ne laser, (3) Lens, (4) Sample, (5) Attenuator, (6) Filter, (7) Photodetector, (8) Oscilloscope [14].

Table 2.1 Thermal Properties vs Thickness of CNT Sample [14]

Tube Length (μm)	12	25	40	46
K_{Au} (W/mK)	268-288	182-243	267-295	250-310
K_{tube} (W/mK)	13-17	12-16.5	13-17	14-17
Thermal diffusivity α_{tube} ($10^{-5}m^2s^{-1}$)	1-2.6	1-10	5-9	0.7-1

Aliev et al. studied the thermal conductivity of three kinds of MWNTs including individual MWNTs, bundled MWNTs and aligned, free-standing MWNTs sheets by both simulations and experiments. They reported a thermal conductivity of 600 ± 100 W/mK for individual CVD grown MWNTs by 3w method that was much lower than the theoretically predicted one. For the bundled MWNTs, a decreased result of 150 ± 15 W/mK for the thermal conductivity was obtained due to quenching of phonon modes which means the transport abilities were weaker compared to the individual MWNTs because the quenching of phonon modes was emphasized by the MWNTs radial deformation. Aligned, free-standing MWNTs sheets, the thermal conductivity was obtained about 50 W/mK due to tube-tube interconnection and sheet imperfection. According to their conclusions, the phonon propagation of MWNTs was better than SWNTs because of the following reasons. First of all, the optical phonon modes were more active since the nanotube diameter of MWNTs was bigger than that of SWNTs, which could enhance heat flow. Second, the intrinsic defects produced by SWNTs were much more severe than those produced by MWNTs. Third, the phonons could get more efficient channels from the neighboring shells in MWNTs to bypass the defective sites than SWNTs. The last reason was MWNTs have more layers of shells so that the inner shells could be protected by the outer shells from the surrounding environment [15].

Juekuan Yang et al. obtained the thermal contact resistance between two individual MWNTs by subtracting the heat resistance of MWNTs from the measured total thermal resistance of two individual contacted MWNTs at room temperature. A result of 10^{-6} W/K of the thermal contact conductance was reported for the aligned contact of MWNTs while 10^{-8} W/K of the contact thermal conductance was reported for the cross contact of MWNTs. Therefore, a contact thermal resistance of 10^{-9} m^2 W/K was reported after normalization [16].

Although most of the research reported the outstanding thermal properties of the CNTs, Prasher reported a range of 0.13 - 0.20 W/mK for the thermal conductivity of the random networks of CNTs. Figure 2.4 show the schematic of the tested random 3-D network of CNTs. ASTM D5470 method was used to measure the thermal conductivity of the samples whose thickness varies from 200-800 μm and two copper rods were used to press the samples in the experiment [9].

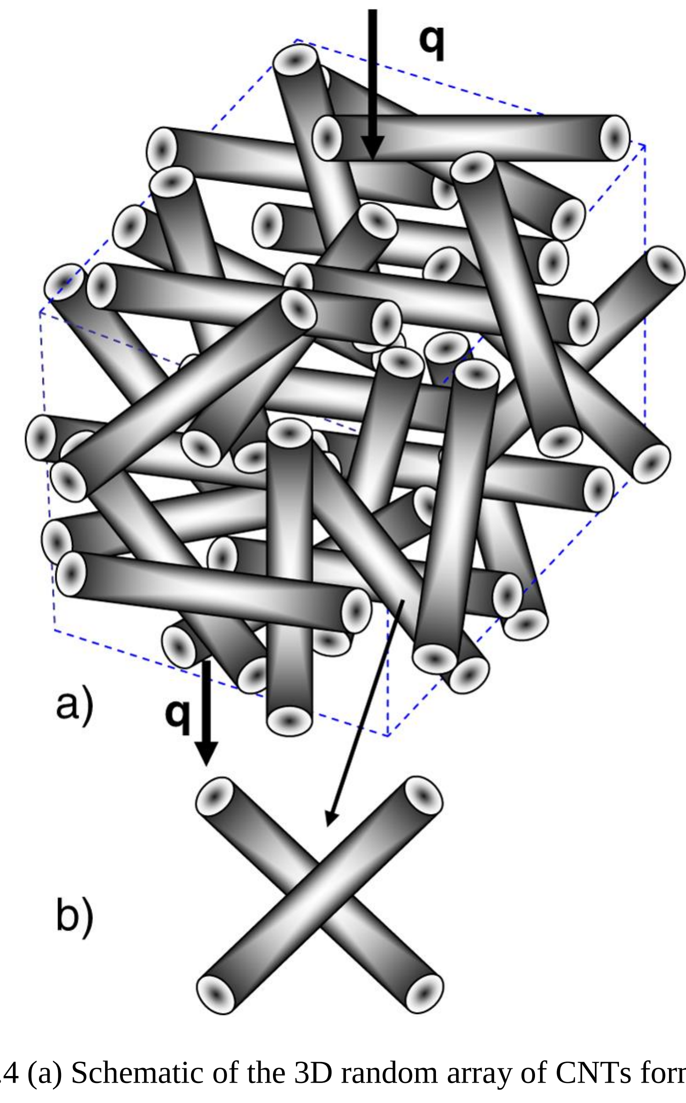

Figure 2.4 (a) Schematic of the 3D random array of CNTs forming a bed.

(b) Schematic of the crossed CNT junction. [9]

Table 2.2 Thermal Conductivity of the CNTs [9]

Sample	Pressure (psi)	K (W/mK)	Volume fraction ϕ
1-2 nm SWNTs	20	0.155	17.2%
	50	0.175	18.1%
	90	0.194	19.4%
<8 nm MWNTs	20	0.154	12.7%
	50	0.171	13.7%
	90	0.195	15.2%
60-100 nm MWNTs	20	0.134	8.9%
	50	0.154	10.4%
	90	0.170	12.4%

All measured data were summarized in Table 2.4. Those samples could be used as thermal insulators according to the experimental results. The thermal conductivity of the samples increased linearly due to the increased volume fraction arising from the increased pressure [9].

Except for the experimental study, many models were established to simulate the theoretical study of CNTs. The model Dr. Pingye Xu used to determine the electrical resistance is called fluctuation-induced tunneling (FIT) [1]. The relationship is:

$$R = R_0 \mathrm{e}^{T_1/(T+T_0)}$$

$$T_0 = 4\hbar S V_0^{3/2} / \pi^2 w^2 k_B \mathrm{e}^2 \sqrt{2\mathrm{m}}$$

$$T_1 = 2 S V_0^2 / \pi k_B \mathrm{e}^2 w$$

S: junction area; w : junction width; V_0: height of the potential barrier; m: electron mass; $\hbar$: reduced Planck constant; R_0: resistance at high temperature [17].

Bor-Woei Huang et al. pointed out that the ballistic thermal conduction should obey the following equation [18]:

$$K_Q = \frac{k_B^2}{h} \sum_m \int_{x_m}^{\infty} dx \frac{x^2 e^x}{(e^x - 1)^2} T_m(\pi^2 k_B^2/\hbar) \approx \frac{\pi^2 k_B^2 T}{3h},$$

Jian et al. used Landauer formula to estimate the relationship between the thermal conductance and temperature [19].

$$G_{th} = \frac{1}{2\pi} \int_0^{\infty} d\omega\, \hbar\omega \mathcal{T}[\omega] \frac{\partial f}{\partial T},$$

Hu and Poulikakos used Fourier's Law to calculate the thermal conductivity which is [20]:

$$\kappa = -\frac{J_Q}{\partial T/\partial z}$$

Those equations are some of the models found to study thermal properties of CNTs, but all of the models were temperature dependent while our experiment is pressure dependent. None of them can be used to determine the test in this thesis. More research might be done for the pressure dependent models of CNTs.

2.2: TIMs

Thermal Interface Materials (TIMs) are another research field which focuses on interfacial thermal resistance. They are also a vital part of research in electronic packing technology. They are materials with high thermal conductivity that can conform to the imperfect mating surfaces by being filled in the voids that can enhance the heat transfer across the interface. The common commercial TIMs we use now includes thermal grease, phase change materials (PCMs), soft metal foils, elastomer paste, thermal putties, adhesives, etc. Their thermal conductivities are ranged from 1 to 10 W/mK. [21]. With the demand for power densities increasing continuously in recent years, the traditional commercial TIMs cannot meet the requirements and show their inefficiency. More advanced TIMs with higher thermal conductivity and easy management needed to be explored.

CNTs are considered as promising candidates for high performance TIMs due to their outstanding thermal, mechanical and electrical properties. Tao et al. used phase sensitive transient thermos-reflectance (PSTTR) technique to measure the thermal conductivity of vertically aligned multiwalled carbon nanotube arrays as TIMs. The thermal Chemical Vapor Deposition (CVD) method was applied to fabricate the MWNTs samples on the silicon wafer. The transition- metal iron was used as a catalyst. Ion beam sputtering method was used to deposit a 10 nm underlayer of aluminum and a 10 nm layer of iron onto the silicon substrate. Molybdenum was also used as an optional underlayer in order to improve the adhesion between MWNTs and silicon substrate. The feedstock was ethylene while the temperature of the fabrication process was around 750 ℃ [21].

The silicon wafer with 100 μm thickness was first measured by both experiment and model calculation because of its acknowledged properties. The measured data and model calculation data was best fit according to the figure they plotted. The heat conduction model they used is shown in Figure 2.5. The first layer as 1 nm thick glass coated with Cr-Au at the inner surface. The middle layer was a 7 μm MWNTs array, and the substrate was a 100 μm thick silicon wafer [21].

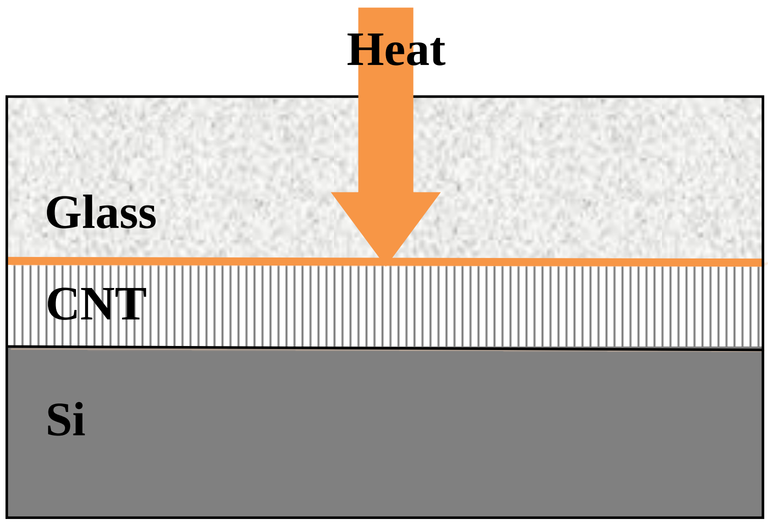

Figure 2.5 Heat Conduction Model [21]

Tong et al. studied thermal interface system by conducting three experiments. The first experiment used the heat conduction model without the top glass layer and let the heating laser contact MWNTs layer directly. The second experiment used the three layer configuration with dry adhesion between MWNTs array and glass surface by van der walls interactions. The third one added a 1 μm indium layer to the Cr/Au coated inner glass surface and welded to MWNTs array thermally. All the model parameters measured from the three experiments were summarized in Table 2.3. And the fixed parameters used in calculation were glass thickness: 1mm, silicon thickness: 100 μm; glass thermal conductivity: 1.06 W/mK, silicon thermal conductivity: 140 W/mK; glass thermal diffusivity: 6.4×10^{-7} m^2/s, silicon thermal diffusivity: 7.4×10^{-5} m^2/s. According to the data, the thermal conductivity of CNT-Si interface was one order of magnitude larger than Glass-CNT interface, and the thermal conductivity could be enhanced by one order of magnitude through welding indium between coated glass and MWNTs arrays. Therefore, more research on dense vertically aligned CNTs as TIMs could be conducted [21].

Table 2.3 Model Parmeters [21]

Model Parameters	Values		
	CNT-Si	Glass-CNT-Si	Glass-In-CNT-Si
Glass-CNT inter. Cond. (W/m^2K)	-	9.0×10^4	3.4×10^6
CNT-Si inter. Cond. (W/m^2K)	2.9×10^6	9.0×10^5	2.2×10^6
CNT cross-plane conductivity (W/mK)	244	265	267
CNT anisotropic ratio	9.0×10^{-3}	1.0×10^{-2}	1.0×10^{-2}
CNT axial diffusivity (m^2/s)	8.4×10^{-4}	3.0×10^{-4}	6.9×10^{-4}
CNT thickness (μm)	4.6	7.0	10.1
Laser heating spot radius (mm)	0.48	0.30	0.46

CNTs as a novel and promising candidate for TIMs application are well accepted nowadays. However, the performance of all CNT TIMs was not same due to various reasons including CNT quality, CNT diameter, array height and density, CNTs adhesion to the growth substrate, etc. There are three kinds of common CNTs array TIMs which are one- sided interface, two-sided interface, and CNT-coated foil interface. The schematic of those three types were shown in Figure 2.6 [22].

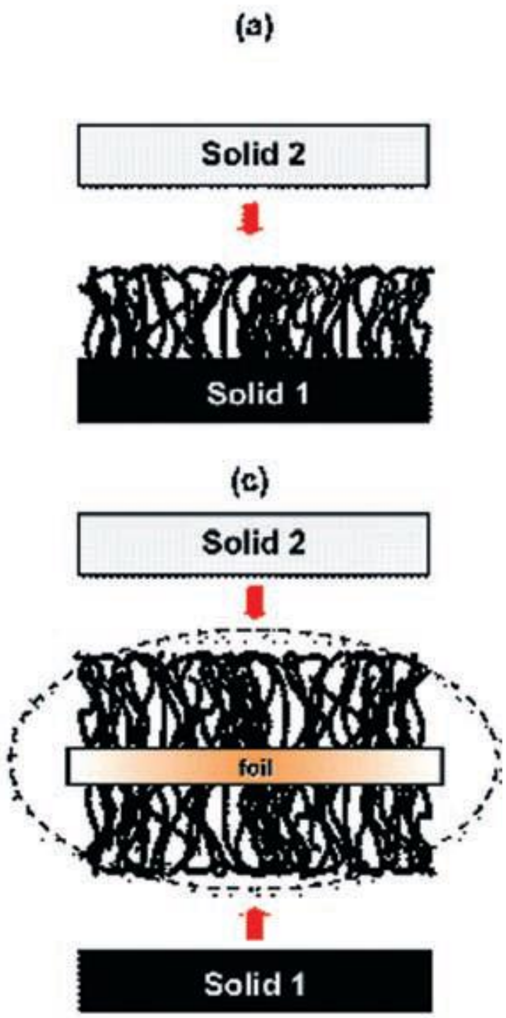

Figure 2.6 CNTs array TIMs interface structures: (a) one-sided interface; (b) two-sided interface, (c) CNT-coated foil interface [22]

The one-sided CNTs array is the most common researched area where CNTs array was grown on the substrate directly. The two-sided configuration consists of two pieces of one-sided configurations and were bonded them by van der waals force. The third configuration was growing CNTs array on both side of a thin foil simultaneously. This kind of structure will first be applied to the interfaces that will be damaged due to high fabrication process temperature that is required for purity and high quality CNT product [22].

The total heat resistance including the resistance of CNT-substrate interfaces at both growth substrate and the opposing interface and the resistance through the CNT array. Comparing with the CNT- substrate interface resistance, the resistance through the CNT array can be neglected when the array height is less than 50 μm. The overall interface resistance can be calculated by scanning electron micrographs of CNTs arrays that can get growth substrate density and estimating real contact area by a model which can get opposing substrate density [23].

If the one-sided CNTs arrays are completely contacted and perfectly matched acoustic impedances at all interface, the theoretical value of the resistance of 0.1 mm^2K/W can be obtained with a surface that have 10^8 CNTs/mm^2density and 20 nm CNT diameters [22]. However, the lowest resistance obtained by Cola's experiment is about 7 mm^2K/W by experiment [24] while the lowest resistance of two-sided interfaces is about 4 mm^2K/W [25]. For the third kinds of configuration, the lowest resistance of the CNT-coated foil TIMs is about 8 mm^2K/W [25].

Using transient method can obtain the CNT-substrate resistances and the CNT array resistance independently [25]. According to those measurements, the results of CNT array resistance is much less than CNT-substrate resistance while the resistance between CNTs and the growth interface of the substrate is also much less than that between CNTs free ends and the opposing substrate. The resistance between CNTs free ends and opposing substrate is the largest in all resistance, which can be clearly seen in Figure 2.7. The same results were also available in two-sided configuration and CNT-coated foil configuration [25] - [26].

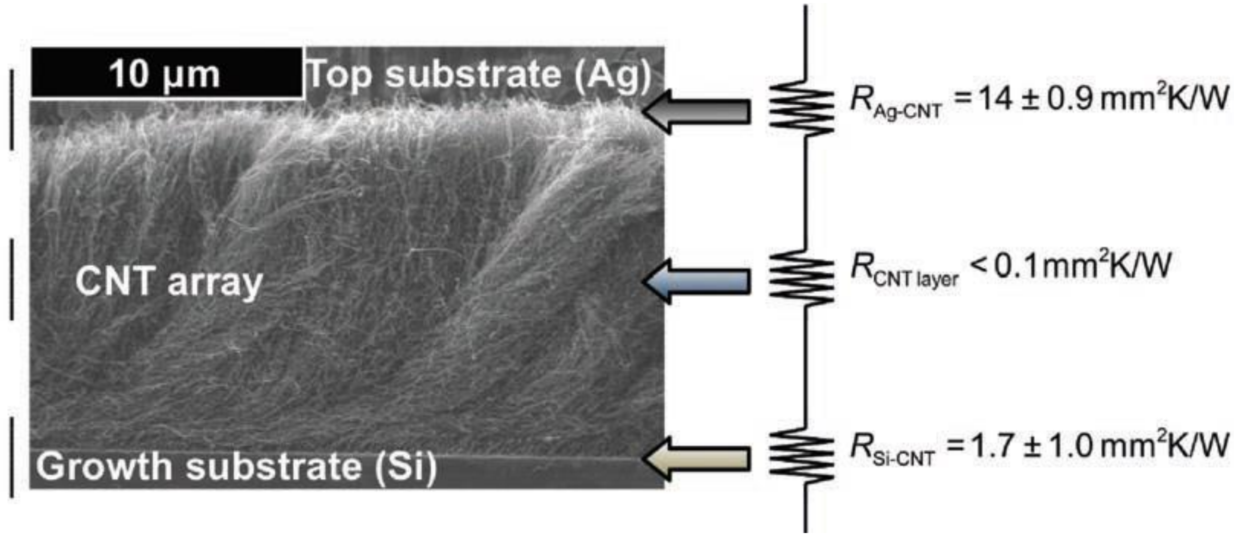

Figure 2.7 True contact resistances for a one-sided Si-CNT-Ag interface at 0.241 MPa measured at room temperature using a photoacoustic technique [25].

An industry burn-in test was applied for CNT-coated foil TIMS by an Intel CPU. One side of the 25 μm thick copper foil was used to grow CNTs. Then the CNTs free ends were contacted heat sink while the other side of the bare foil was contacted with the die directly. The resistances produced by the tested TIMs were 30% lower than that of bare foil TIMs by 1000 thermo-mechanical cycles [27].

Chapter 3

Test Setup and Results

3.1 Fabrication Method and Sample Preparation

There are several common ways to fabricate the CNTs nowadays such as Chemical Vapor Deposition (CVD), inkjet printing [28], electrophoretic deposition (EPD) [29] etc. Due to its simplicity, economy and fewer restrictions, CVD is the most common fabrication method of growing CNTs directly on a substrate from hydrocarbon vapors. Additionally, compared to all other methods, the production of CNTs by CVD is more controllable, and the purity of the CNTs is higher. However, there is one shortcoming of this method, which is the high temperature between 600 ℃ to 1200 ℃ that is required by the production process [30]. Therefore, the electrical and mechanical properties of CNTs can be negatively influenced which could make CNTs not suitable as a material for some electronic components and applications. [31].

Xu et al. found a solution-based fabrication method, which can be applied at room temperature whereby the shape easily controlled as well as placing the material precisely. The purity of the CNTs post fabrication was shown to be the same by Raman spectroscopy and the electrical characterization was verified to be as expected by both experiment [1] and FIT model [1].

In this research, a same fabrication method of Xu et al. was applied in order to study the thermal interfacial jump between surfaces. Besides CNTs, sodium dodecyl sulfate (SDS) was needed to help CNTs disperse into deionized (DI) water as a surfactant. Both MWNTs and SDS were bought from Sigma-Aldrich. According to the process, the fabrication was followed the steps below:

1. Add 0.4 wt% SDS to DI water and stir for 10 mins to make sure the mixture fully dissolved.
2. Add 0.4 wt% MWNTs to the dissolved solution and stir for 10 mins.
3. Use a tip sonicator to disperse the solution for 60 mins with an amplitude of 40%.
4. Put the tip sonicator in an ice bath and pause the vibration for 5s every 5s.
5. Centrifuge the solution for 30 mins at 3000 rpm.
6. Collect the supernate and stored at 10 ℃.
7. Put the substrate in a liquid–tight frame.
8. Pour the supernate into the frame.
9. Place the whole structure into a vacuum system.
10. Evacuate and vent at 5 kPa for three times.
11. Remove the structure from the vacuum system, put it in a vented box, then heat it at 50 ℃ to evaporate.
12. After evaporating, the product should look similar to the copper disc with CNTs film in Figure 3.1 (a)

The substrates were chosen to be the copper disks that were used for Thermal Interface Material (TIM) tester. The Testing method will be explained in Chapter 3.2. The bare copper disk sample is also shown in Figure 3.1 (b).

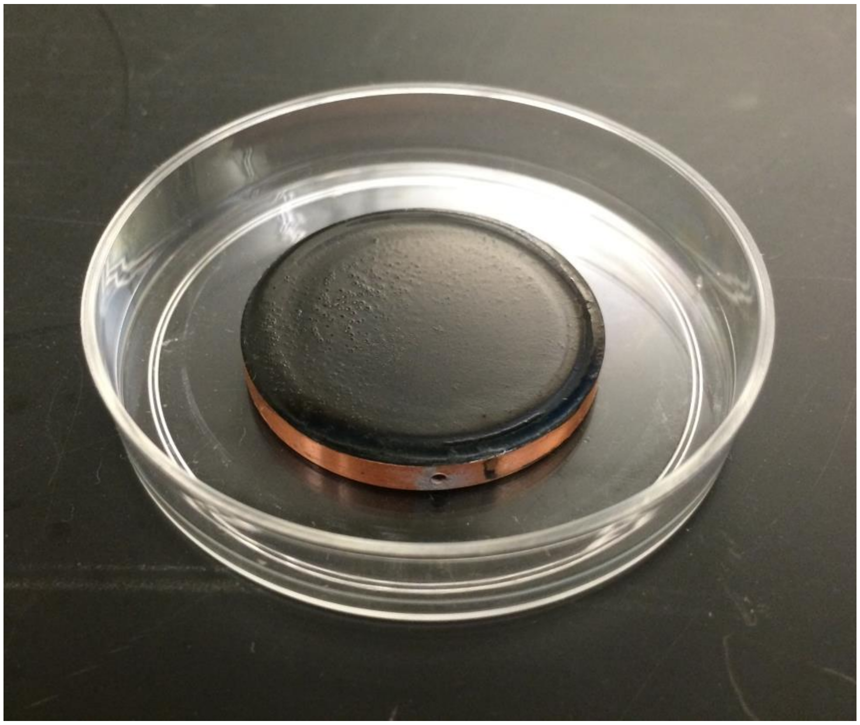

(a)

(b)

Figure 3.1 (a) Copper Disk with CNTs film

(b) Bare Copper Disk Sample

3.2 Test methodology

Again, the purpose of this study was to determine the interfacial thermal resistance of this class of solution deposited CNT films once applied. It is known that the electrical conductivity is high as shown by Xu and Hamilton [1] . However, no good known models exist to predict the thermal resistance of these CNT bumps. Therefore, a series of these bumps were tested as traditional TIMs. Materials would be tested in order to quantify their thermal behavior.

In order to measure the thermal interfacial resistance, a method of measuring the temperature difference across a constant area per heat flux across the interface was used. In this thesis, ASTM D5470 which is a very common and widely accepted standard for the thermal interfacial resistance research was chosen. According to that standard, there are two meter bars in the testing apparatus where the heat is provided from the one meter bar while the other one is cooled. The testing sample is placed between those two meter bars. Several temperature sensors are equipped in each meter bar in order to measure the drop across the sample. The thickness of the sample at the interface was assumed being uniform and the heat flow is assumed being uniform, one dimensional without lateral heat spreading and perpendicular to the test surface [32].

A TIM Tester Model 1400 with ASTM D5470 from Analysis Tech. was used which showed in Figure 3.2 (a). Figure 3.2 (b) shows the detailed testing set up. The Alloy 110 copper disks (shown in Figure 3.1) were used as the substrates since CNTs cannot be tested directly. The heat was provided by the upper meter and the cold was provided by chiller through the lower meter. The range of the applied pressure is from 5 to 95 psi with an accuracy of ±2.5 psi. The flatness of the testing surface is 7-8 micron and the surface is highly smooth with nickel polished finish. The foam insulating sleeves used to minimize the heat loss to the surroundings. Two high

(a)

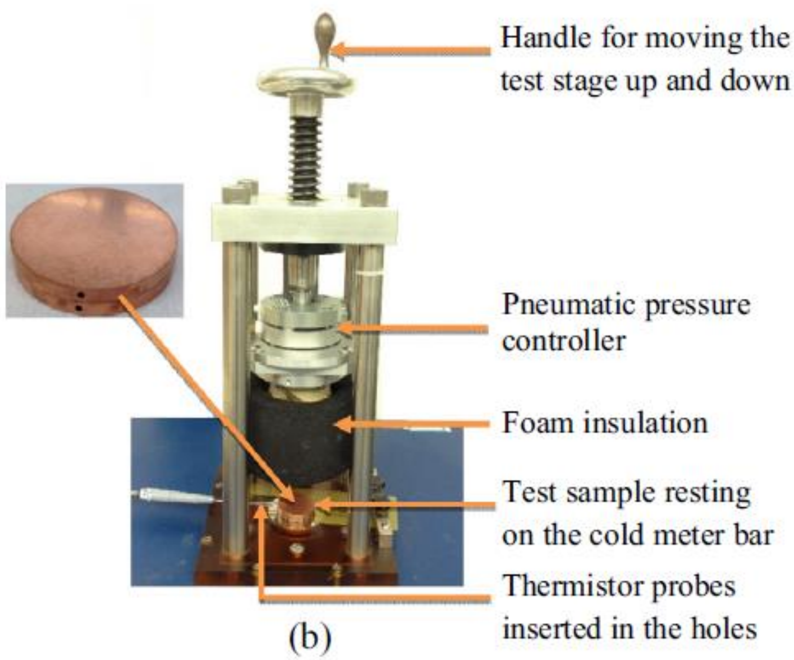

Figure 3.2 (a) TIM Tester Model 1400 by Analysis Tech Inc. Website

(b) Testing of sample using modified test rig; the copper disks was placed between the TIM tester surfaces [33] precision thermistor probes with 1 mm diameter and an accuracy of 0.05 ℃ were inserted into the drilled hole with 1.2 mm diameter located in the middle of the copper disk (shown in Figure 3.1(b)) to measure the temperature differential of the CNT films. Thermal grease (TGREASE 880 by Laird Technologies) filled in the hole in order to reduce the contact resistance of the probes. Before inserting the probes, silicon oil (PMX-200 fluid by Xiameter, viscosity 1000 CS) was applied to the hole in order to reduce the air and decrease the contact resistance. The same silicon oil was applied to the top and bottom of the samples which are the surface contact with upper metal and lower metal with same reason [33]. Using the Analysis Tech WinTIM Software v7.2.0, the heat flux through the samples can also be determined.

All contact interfaces including samples and tester surfaces needed to be cleaned in order to minimize the influence of contaminants. Figure 3.3 shows the target location of the disk by using a specific ruler in order to make sure that the sample will be on the center of the base. Then the ruler will be removed and the upper meter will contact with the top interface of the sample by rotating the handle. The silicon oil or the thermal grease needed to be removed if they exceeded from the drilled holes or the contact interfaces before the tests begins. Figure 3.4 shows the apparatus used in this experiment.

The temperature of upper disk T_1 and the temperature of lower disk T_2 were measured by two thermistors so the temperature difference ΔT was calculated by Equation 3.5. The area A of the Alloy 110 disk was 8.55 cm^2, and the heat energy Q was measured by the software so that the heat flux Q'' was calculated by Equation 3.6. Therefore, the total heat resistance R between two centers of the sample was calculated by Equation 3.7. In order to get the heat resistance of CNTs R_{CNTs}, the heat resistance of the disk R_{disk} needed to be subtracted. R_{disk} was calculated by Equation 3.8. The length L (half of the disk thickness) was 1.6mm, and the thermal conductivity

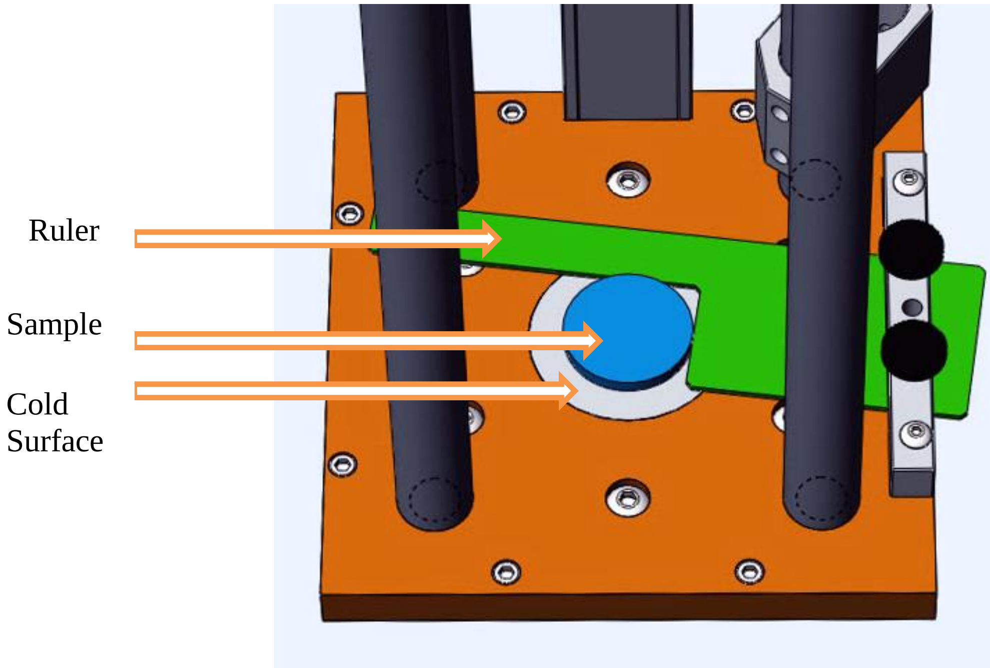

Figure 3.3 Positioning with the Alignment Fixture copy from Analysis Tech Inc. Website

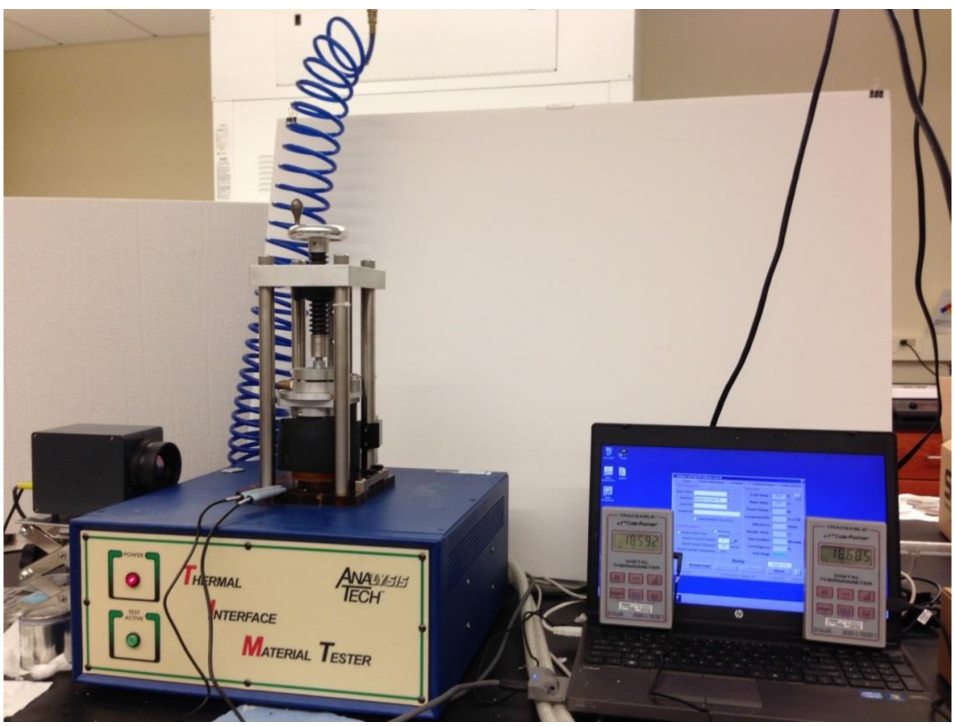

Figure 3.4 TIM Tester Model 1400 with Thermistors and Analysis Tech WinTIM Software

v7.2.0 (test on running)

K_{disk} of the disk was 388 W/mK. Therefore, the result of the R_{disk} was 0.082 cm^2K/W, so that the R_{CNTs} can be calculated by Equation 3.9. Figure 3.6 shows the schematic of the calculation.

$$\Delta T = T_1 - T_2 \tag{3.5}$$

$$Q'' = Q/A \tag{3.6}$$

$$R = \Delta T/Q'' \tag{3.7}$$

$$R_{disk} = 2L/K_{disk} \tag{3.8}$$

$$R_{CNTs} = R - R_{disk} \tag{3.9}$$

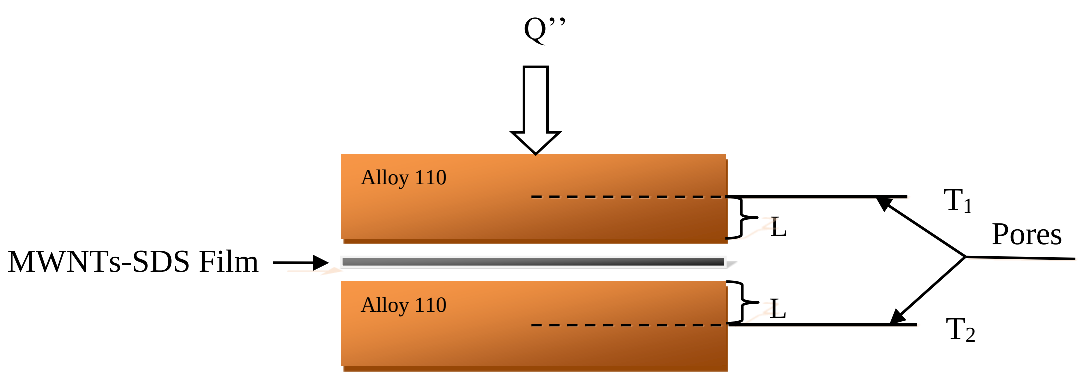

Figure 3.5 Representative Schematic of Calculations Used for Data Reduction

3.3 Results

By controlling the volume of the solution used in the fabrication process, three groups of samples were tested under 20 psi, 40 psi, 60 psi, 80 psi respectively. Every tested was repeated 10 times continuously under each pressure in order to remove any data scatter. The detail category of all groups is shown in Table 3.1. All tests were run at 348.15K (75 ℃) for at least 30 minutes and then cooled back until the core temperature was less than 303.15K (30 ℃).

Table 3.1 Groups of Sample

	Group 1	Group 2 (Single Sided)				Group 3 (Double Sided)		
Volume of the Solution	Bare	2 mL	4 mL	6 mL	8 mL	4 mL	8 mL	12 mL

Figure 3.7, Figure 3.8 and Figure 3.9 shows representative schematic of three different groups. Table 3.2 – 3.9 shows the data results. The data analysis will be discussed in the chapter 4.

Group 1: Bare Alloy 110 Disk

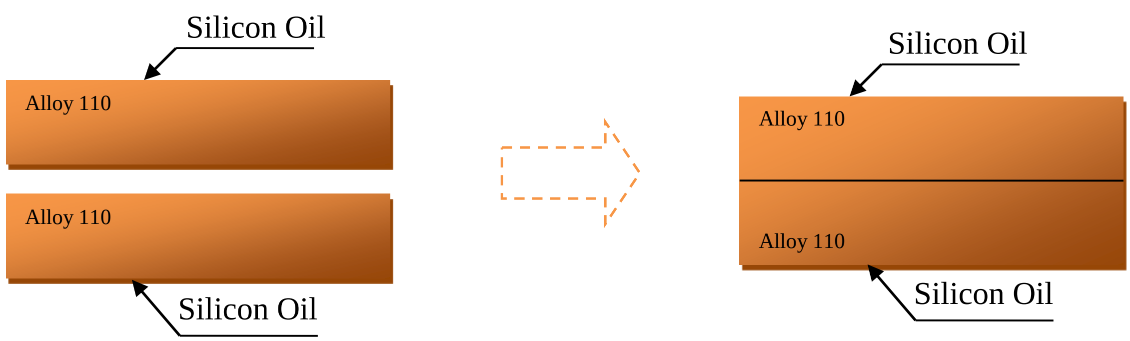

Figure 3.6 Representative Schematic of Bare Alloy 110 Disk Sample

Figure 3.7 Heat Resistance for Bare Sample

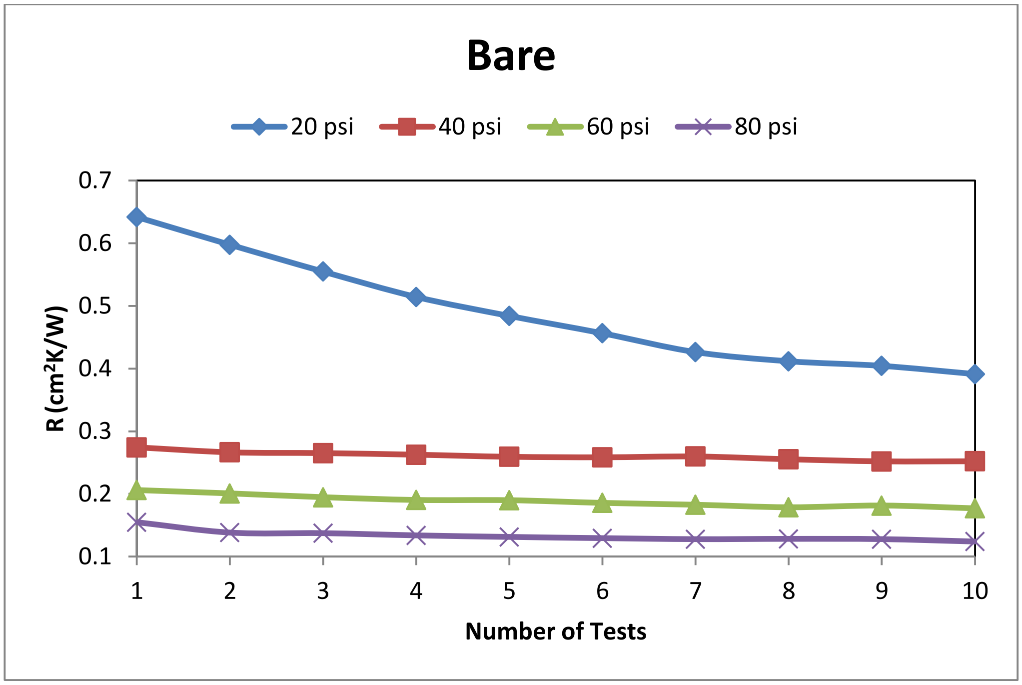

Group 2: Single Sided CNTs Printed Sample

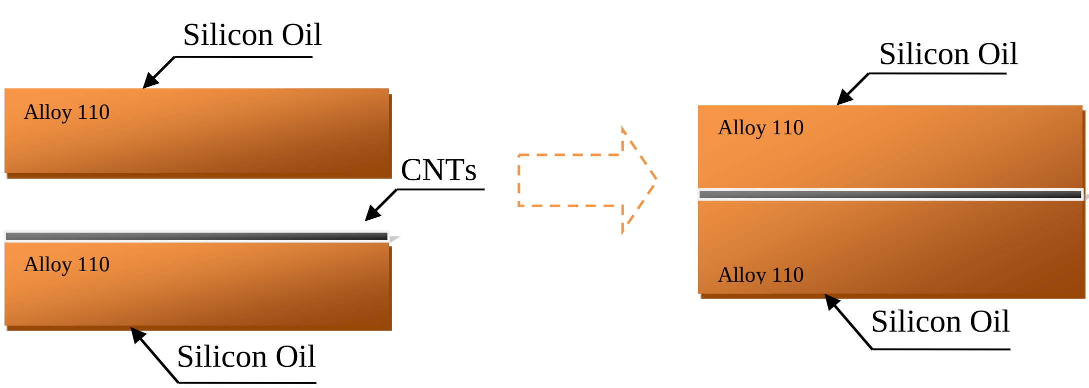

Figure 3.8 Representative Schematic of Single Sided CNTs Printed Alloy 110 Disk Sample

Figure 3.9 Heat Resistance for Single Sided Sample Printed 2 mL CNTs

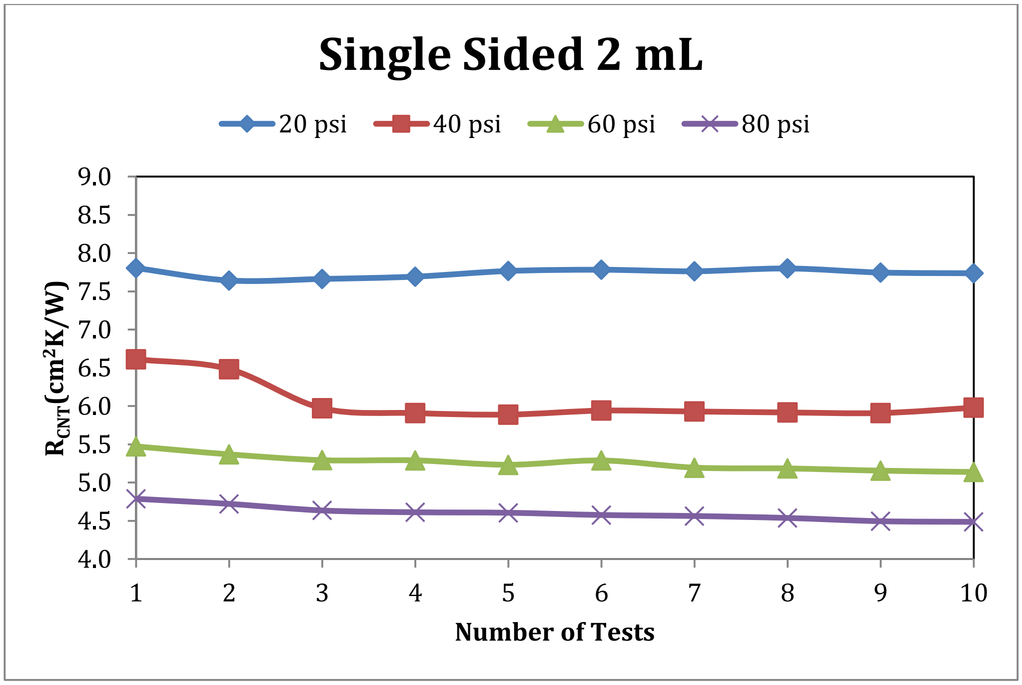

Figure 3.10 Heat Resistance for Single Sided Sample Printed 4 mL CNTs

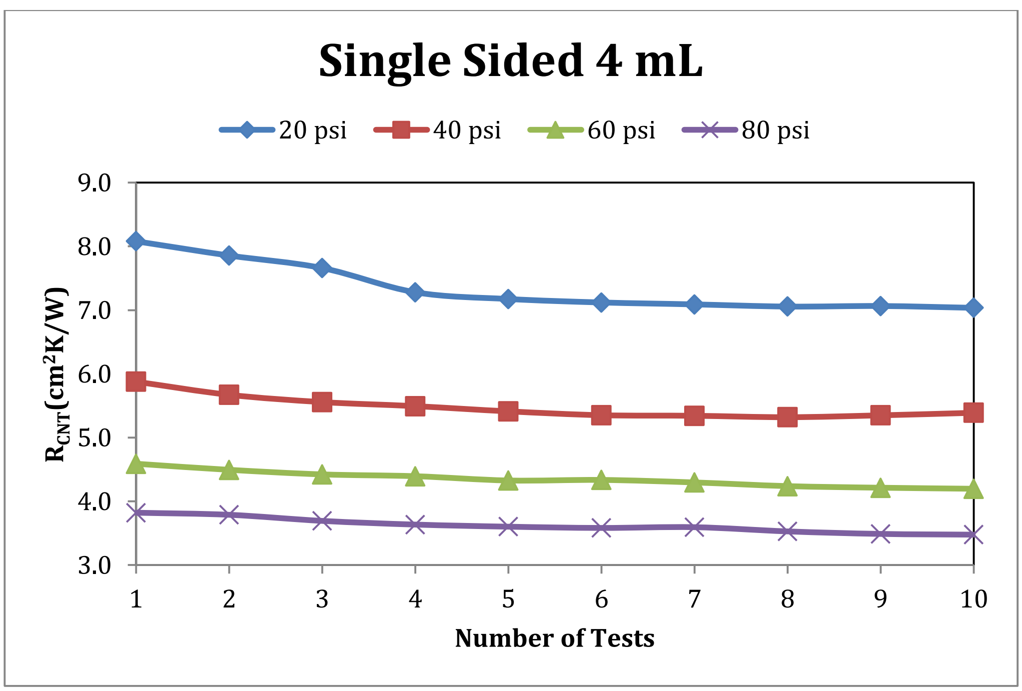

Figure 3.11 Heat Resistance for Single Sided Sample Printed 6 mL CNTs

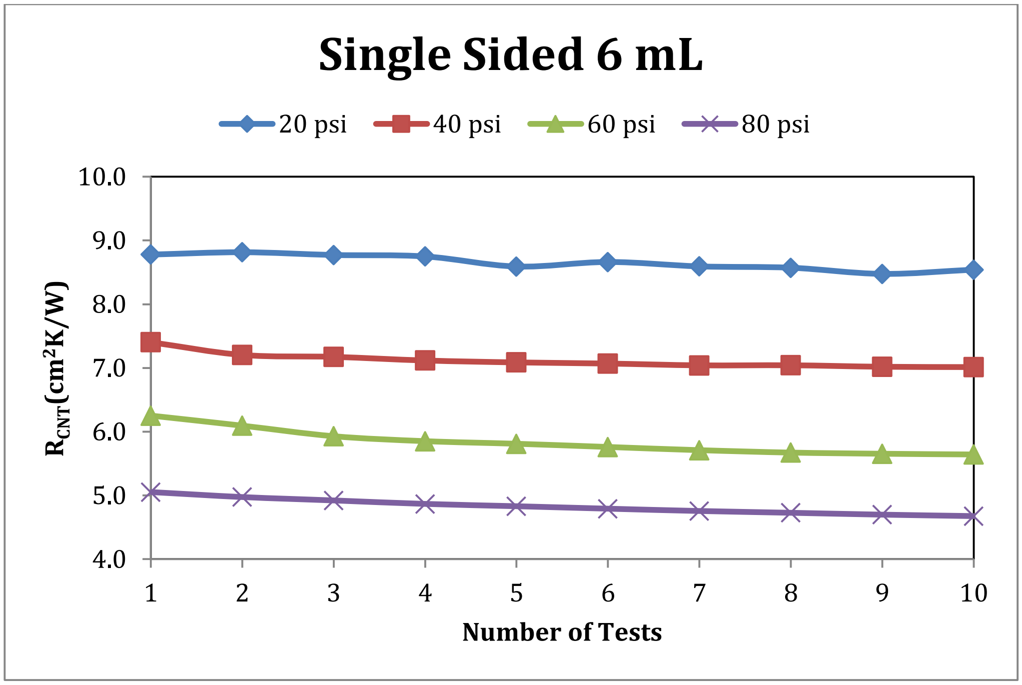

Figure 3.12 Heat Resistance for Single Sided Sample Printed 8 mL CNTs

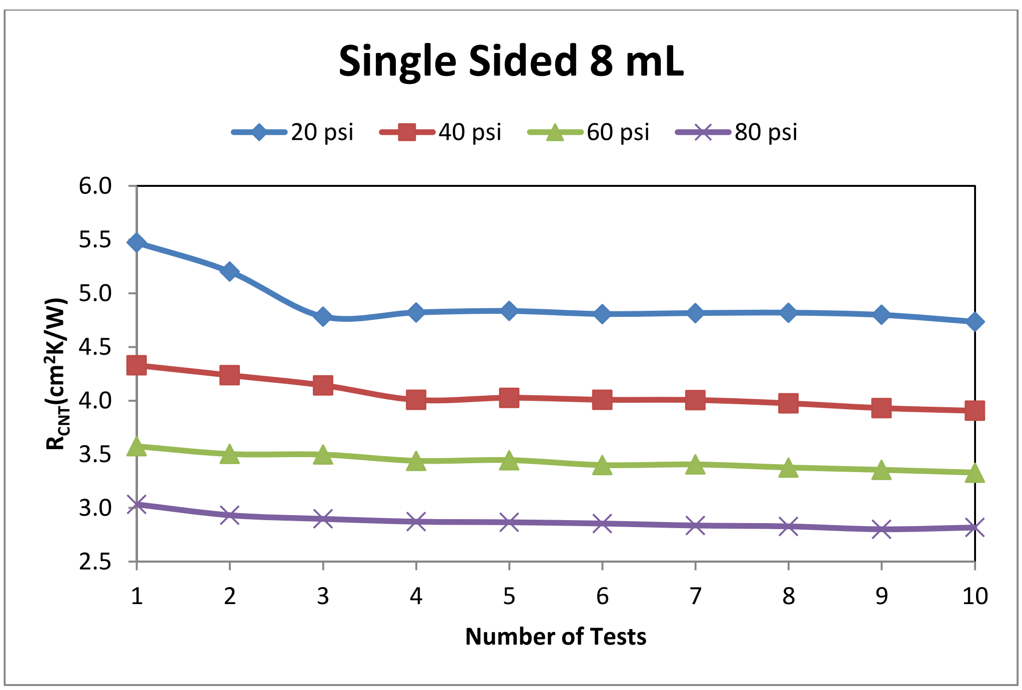

Group 3: Single Side CNTs Printed Sample

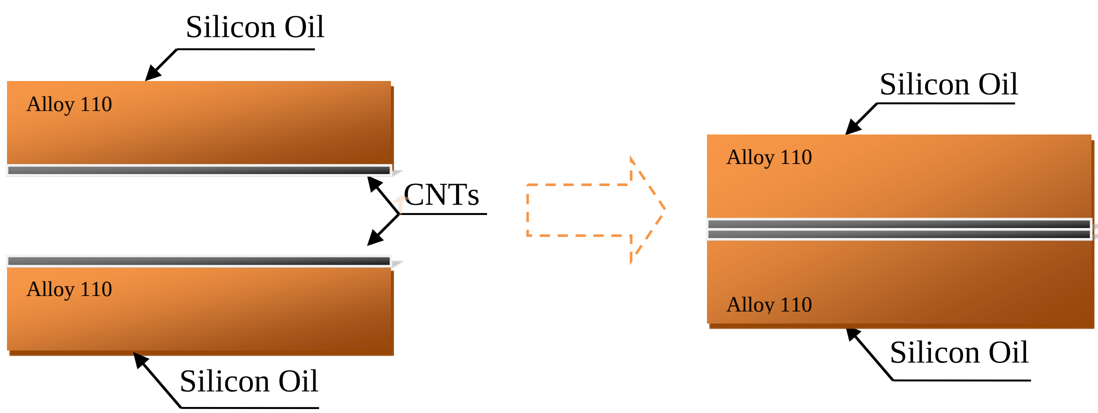

Figure 3.13 Representative Schematic of Double Sided CNTs Printed Alloy 110 Disk Sample

Figure 3.14 Heat Resistance for Double Sided Sample Printed 4 mL CNTs

(2 mL CNTs printed each)

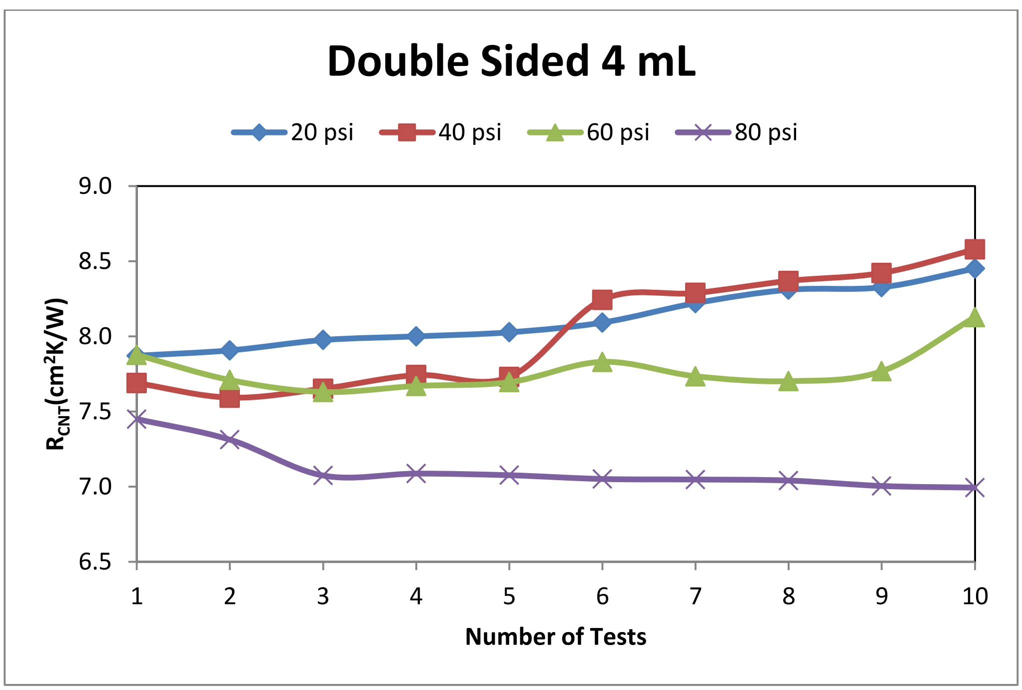

Figure 3.15 Heat Resistance for Double Sided Sample Printed 8 mL CNTs

(4 mL CNTs printed each)

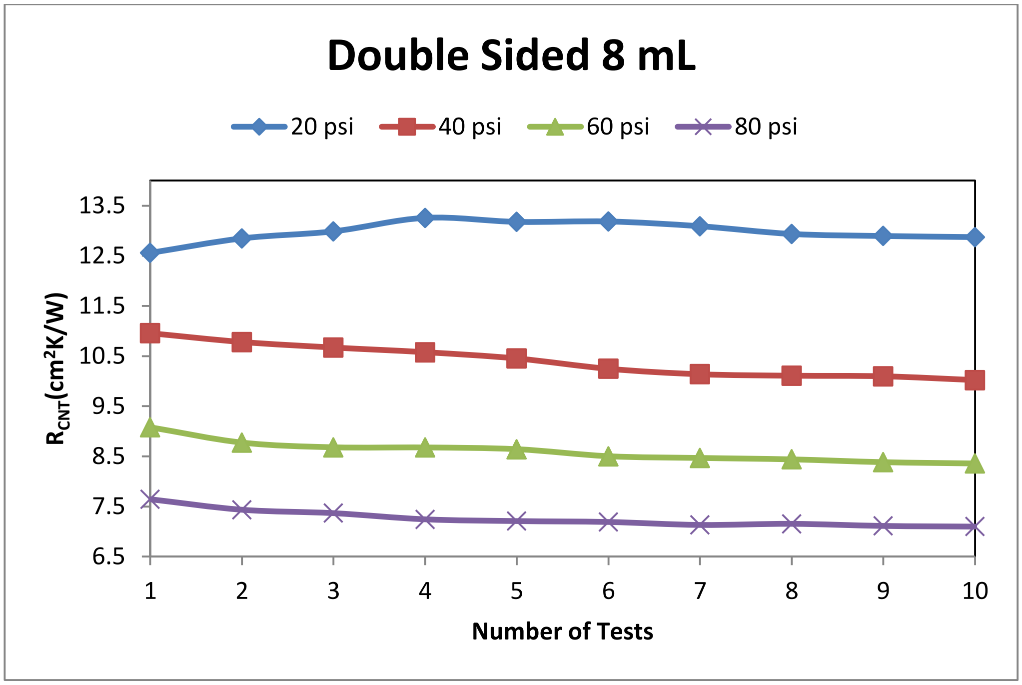

Figure 3.16 Heat Resistance for Double Sided Sample Printed 12 mL CNTs

(6 mL CNTs printed each)

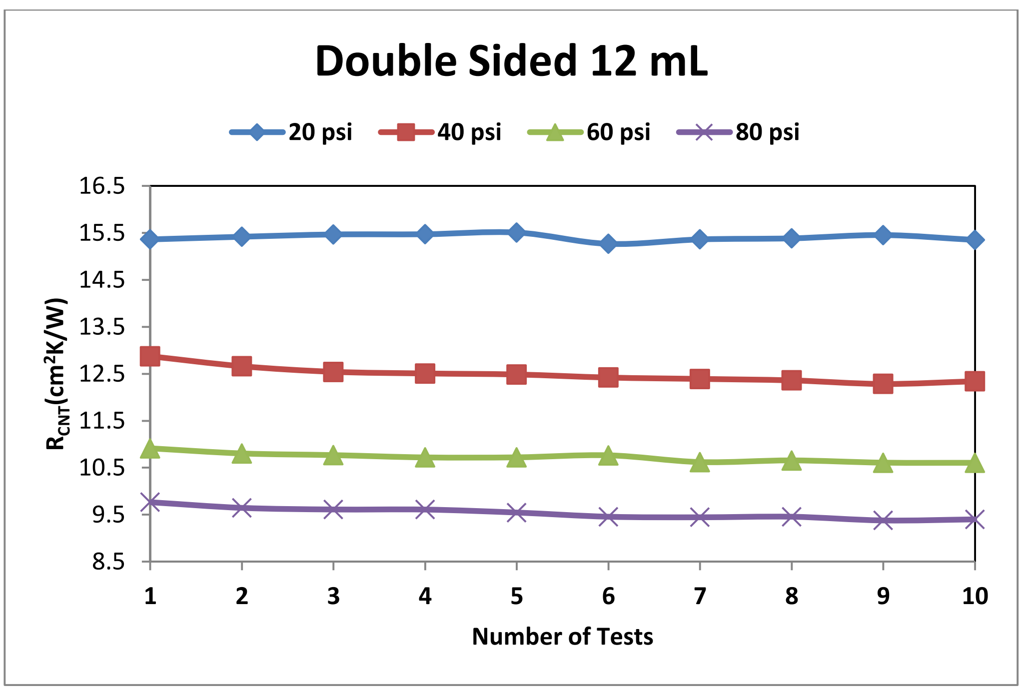

The average values of last five single set of tests were summarized in Table 3.10. More detail analysis would be discussed in Chapter 4.

Table 3.2 Average Heat Resistance of Last Five Measurements

		Group 1	Group 2 (Single Sided)				Group 3 (Double Sided)		
		Bare	2 mL	4 mL	6 mL	8 mL	4 mL	8 mL	12 mL
Average Heat Resistance (cm^2K/W)	20 psi	0.418	7.715	7.073	8.57	10.379	8.28	12.996	15.364
	40 psi	0.255	5.963	5.35	7.037	8.662	8.38	10.122	12.359
	60 psi	0.181	5.127	4.256	5.688	7.807	7.833	8.43	10.651
	80 psi	0.127	4.468	3.534	4.73	7.081	7.027	7.137	9.427

Chapter 4

Analysis and Comparison

As mentioned before, three groups of samples were tested by an Analysis Tech TIM Tester Model 1400 using the ASTM 5470 method. Every single sample was tested continuously ten times under four different of pressures, 20 psi, 40 psi, 60 psi, and 80 psi in order to make sure the test results were obtained under steady state and remove any data scatter. Therefore, the last five values were chosen to calculate the average thermal interfacial resistance. The average thermal interfacial resistances of all samples are shown by column chart through Figure 4.1- Figure 4.8 The values of average heat resistance, standard deviation, positive error and negative error of all tests are summarized through Table 4.1-Table4.8. The data range was represented by the error bar in every column chart. The positive error value is the difference between the maximum values and the average values and the negative error value is the difference between the minimum values and the average values.

The maximum standard deviation among all sets of tests is 0.082 and the biggest positive error is 0.259 while the maximum negative one is 0.158 which are small enough to be ignored since the tested heat resistances of all CNT films are very high. According to the uncertainty analysis from Roy et al [33], the uncertainties of all results in this thesis are less than 5%, which are negligible. Therefore, the average thermal interfacial resistances of all samples are reliable and they could be the representative of every single set test results. It also could be seen very clear from the small error bar on Figure 4.1-Figure 4.8. Therefore, the average values were used to be compared instead of all data.

Table 4.1 Error Analysis of Bare Copper Disk

	Group 1 Bare			
	Average Heat Resistance (cm^2K/W)	Standard Deviation	Positive Error Value	Negative Error Value
20 psi	0.418	0.025	0.038	0.027
40 psi	0.255	0.004	0.005	0.003
60 psi	0.181	0.003	0.005	0.004
80 psi	0.127	0.002	0.002	0.003

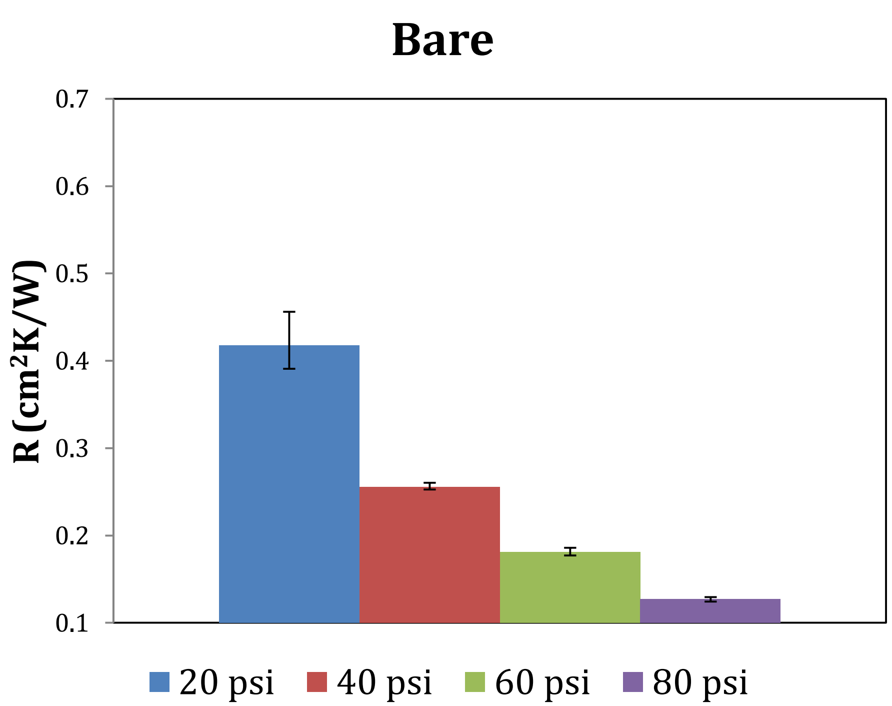

Figure 4.1 Average Thermal Resistance of Bare Copper Disk

Table 4.2 Error Analysis of Single Sided 2 mL of CNT Films

	Group 2 Single Sided 2 mL			
	Average Heat Resistance (cm^2K/W)	Standard Deviation	Positive Error Value	Negative Error Value
20 psi	7.715	0.014	0.011	0.017
40 psi	5.963	0.036	0.044	0.04
60 psi	5.127	0.016	0.026	0.021
80 psi	4.468	0.018	0.029	0.016

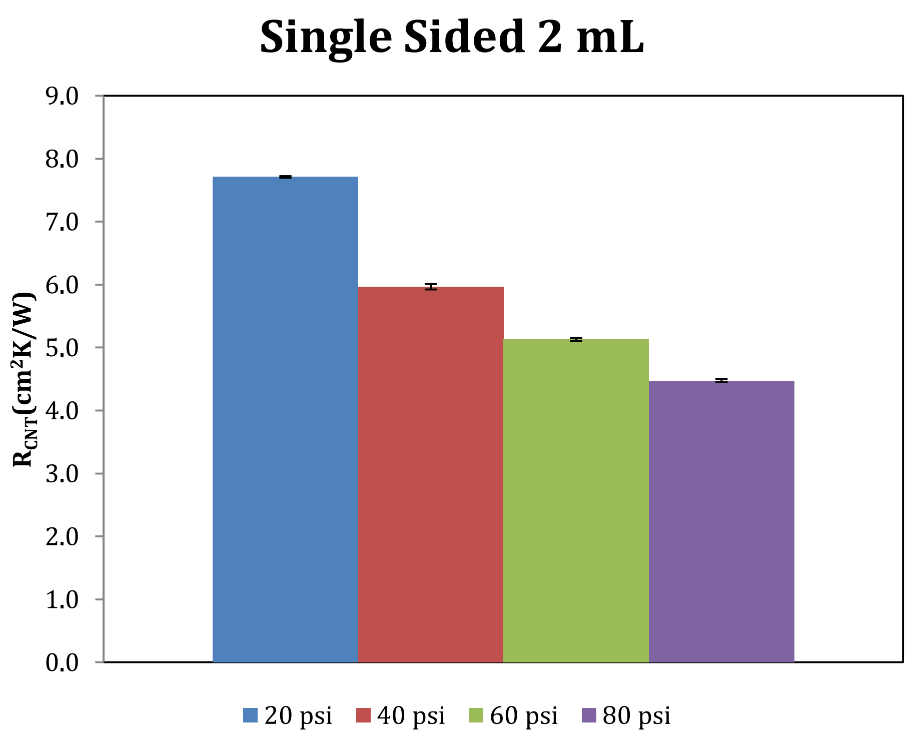

Figure 4.2 Average Thermal Resistance of Single Sided 2 mL of CNT Films

Table 4.3 Error Analysis of Single Sided 4 mL of CNT Films

	Group 2 Single Sided 4 mL			
	Average Heat Resistance (cm^2K/W)	Standard Deviation	Positive Error Value	Negative Error Value
20 psi	7.073	0.033	0.047	0.037
40 psi	5.35	0.025	0.039	0.03
60 psi	4.256	0.058	0.08	0.059
80 psi	3.534	0.053	0.06	0.057

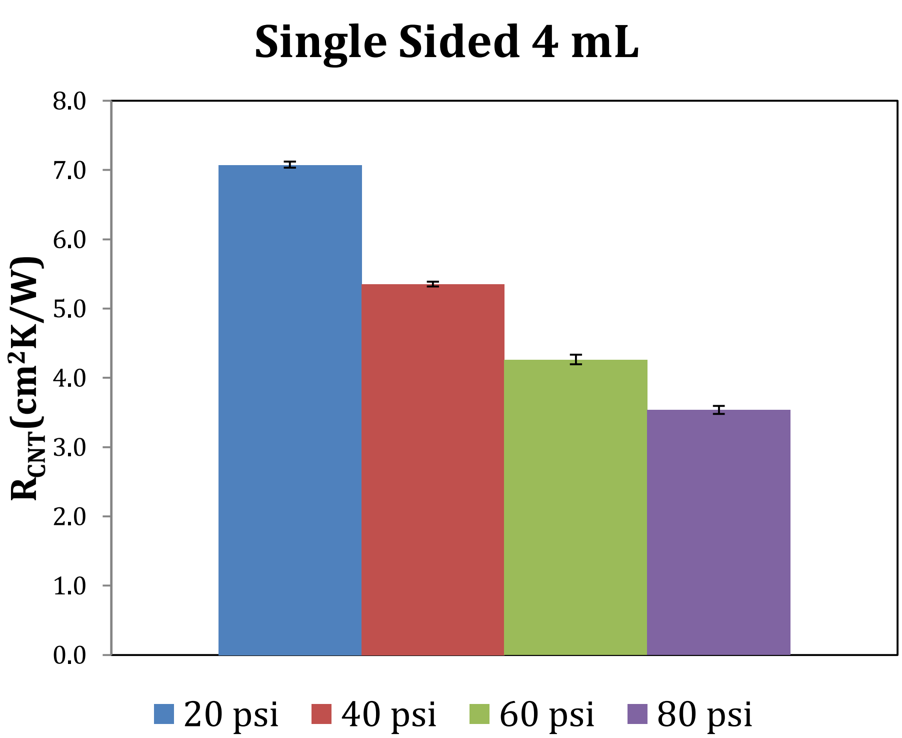

Figure 4.3 Average Thermal Resistance of Single Sided 4 mL of CNT Films

Table 4.4 Error Analysis of Single Sided 6 mL of CNT Films

	Group 2 Single Sided 6 mL			
	Average Heat Resistance (cm^2K/W)	Standard Deviation	Positive Error Value	Negative Error Value
20 psi	8.570	0.068	0.093	0.094
40 psi	7.037	0.022	0.032	0.023
60 psi	5.688	0.048	0.073	0.045
80 psi	4.730	0.046	0.062	0.054

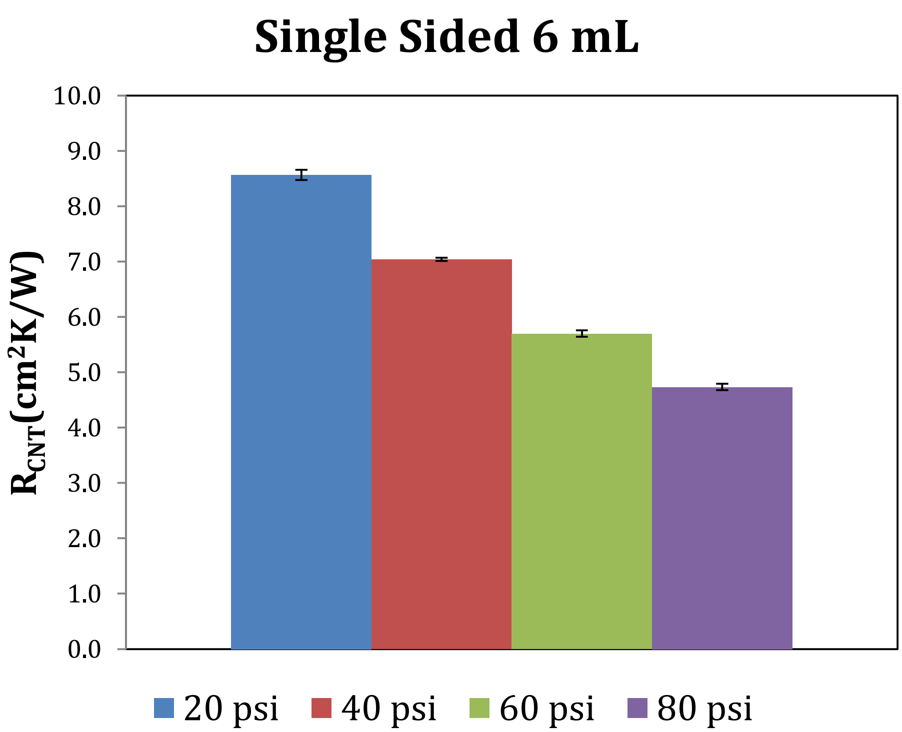

Figure 4.4 Average Thermal Resistance of Single Sided 6 mL of CNT Films

Table 4.5 Error Analysis of Single Sided 8 mL of CNT Films

	Group 2 Single Sided 8 mL			
	Average Heat Resistance (cm^2K/W)	Standard Deviation	Positive Error Value	Negative Error Value
20 psi	10.379	0.026	0.043	0.024
40 psi	8.662	0.045	0.066	0.05
60 psi	7.807	0.020	0.022	0.026
80 psi	7.801	0.030	0.046	0.026

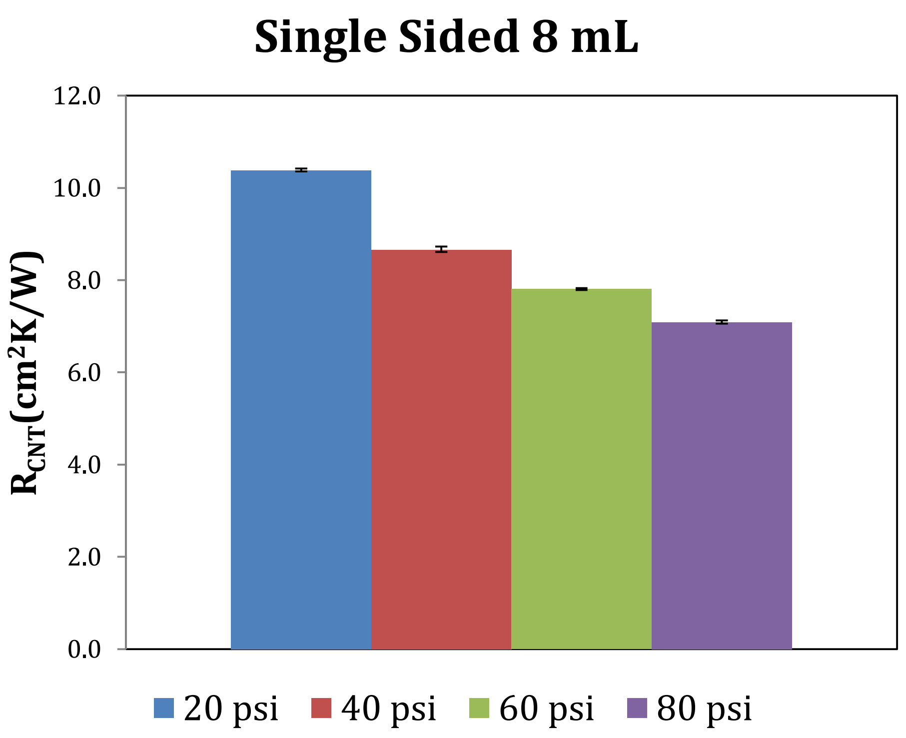

Figure 4.5 Average Thermal Resistance of Single Sided 8 mL of CNT Films

Table 4.6 Error Analysis of Double Sided 4 mL of CNT Films (2 mL Each Side)

	Group 3 Double Sided 4 mL			
	Average Heat Resistance (cm^2K/W)	Standard Deviation	Positive Error Value	Negative Error Value
20 psi	8.28	0.134	0.171	0.158
40 psi	8.38	0.131	0.198	0.137
60 psi	7.833	0.172	0.295	0.131
80 psi	7.027	0.027	0.024	0.034

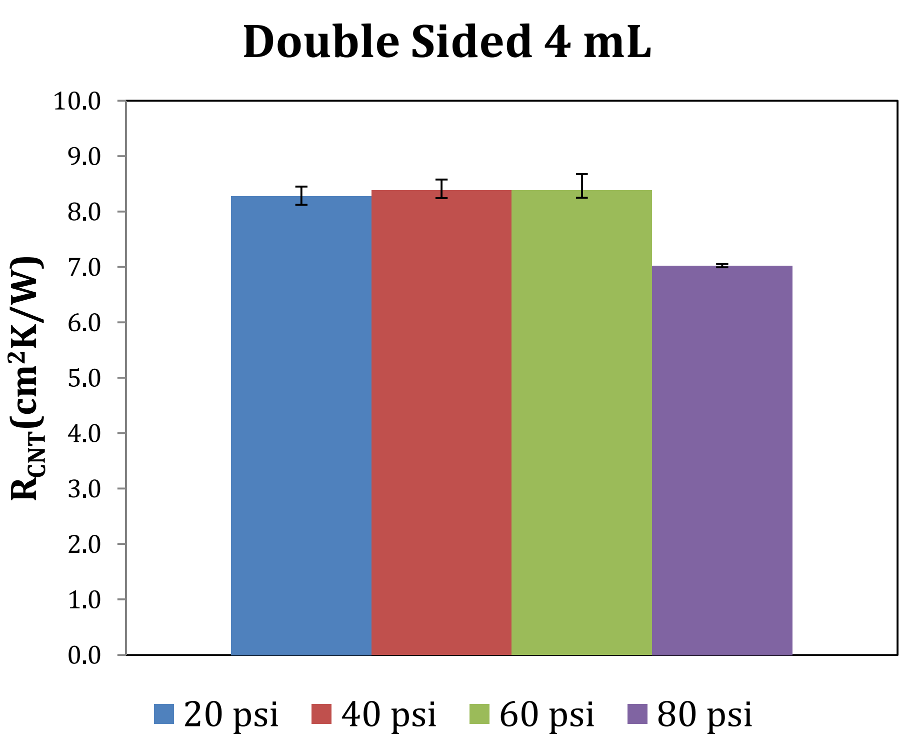

Figure 4.6 Average Thermal Resistance of Double Sided 4 mL of CNT Films (2 mL Each Side)

Table 4.7 Error Analysis of Double Sided 8 mL of CNT Films (4 mL Each Side)

	Group 3 Double Sided 8 mL			
	Average Heat Resistance (cm^2K/W)	Standard Deviation	Positive Error Value	Negative Error Value
20 psi	12.996	0.136	0.189	0.123
40 psi	10.122	0.082	0.123	0.102
60 psi	8.43	0.060	0.072	0.073
80 psi	7.137	0.036	0.053	0.039

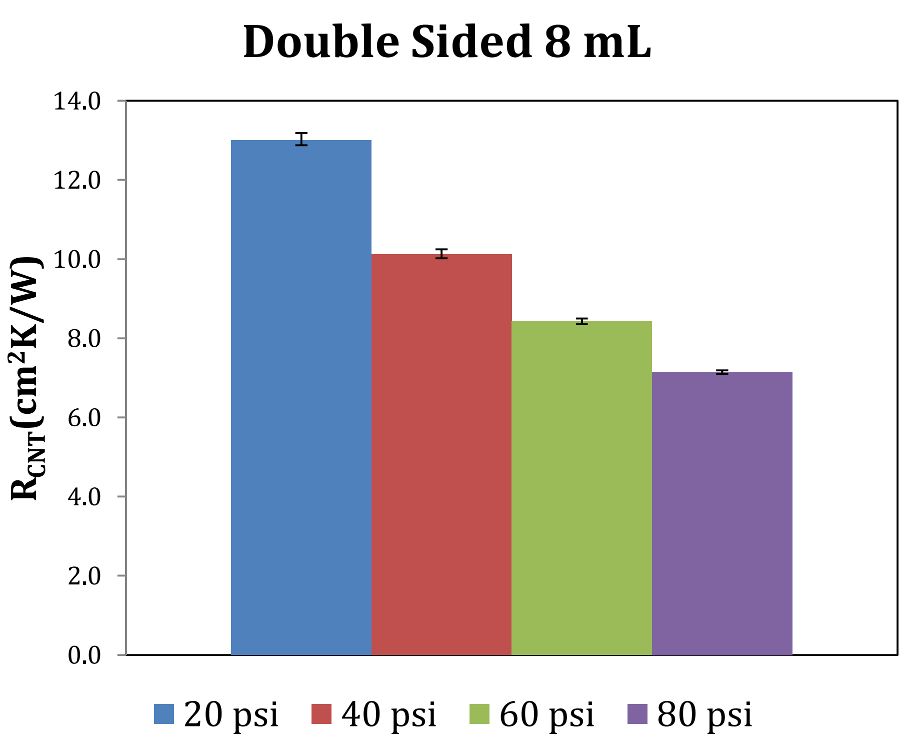

Figure 4.7 Average Thermal Resistance of Double Sided 8 mL of CNT Films (4 mL Each Side)

Table 4.8 Error Analysis of Double Sided 12 mL of CNT Films (6 mL Each Side)

	Group 3 Double Sided 12 mL			
	Average Heat Resistance (cm^2K/W)	Standard Deviation	Positive Error Value	Negative Error Value
20 psi	15.364	0.067	0.091	0.097
40 psi	12.359	0.052	0.061	0.076
60 psi	10.651	0.067	0.113	0.046
80 psi	9.427	0.036	0.029	0.05

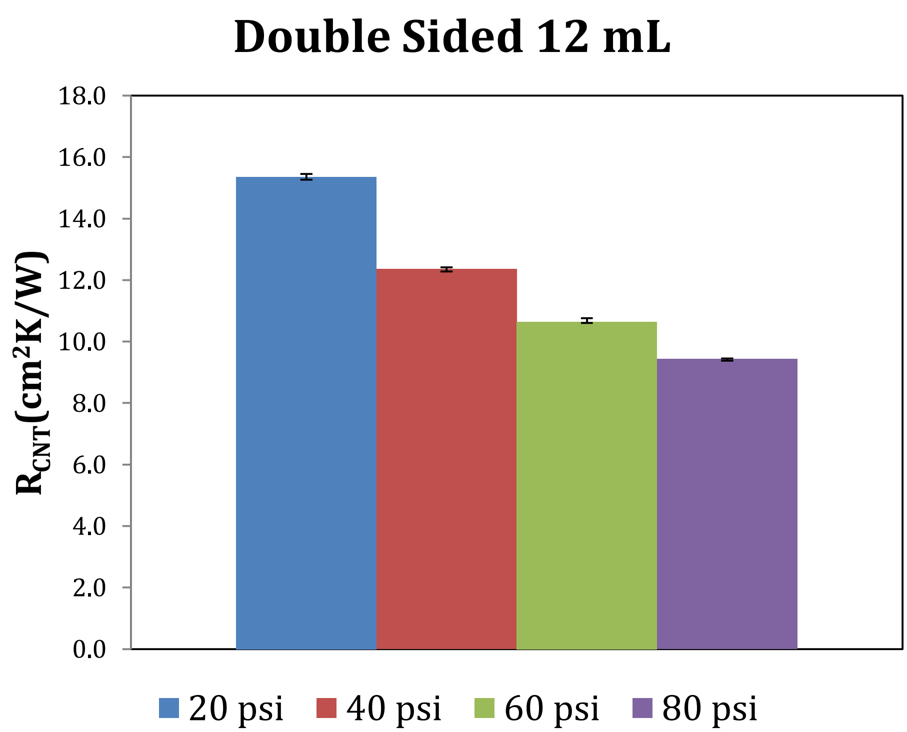

Figure 4.8 Average Thermal Resistance of Double Sided 12 mL of CNT Films (6 mL Each Side)

The thermal conductivity is an important property among all kinds of thermal properties for the solid materials which was highly influenced by thermal interfacial resistance. According to the average values of thermal resistance of the CNT films from Table 3.10, a result of very high thermal interfacial resistances was obtained. This result showed that the solution deposited CNT films fabricated by Xu et al.'s method could perform as thermal insulators. However, excellent electrical properties were reported by Xu et al. Therefore, the application of this kind of solution deposited CNT films might be the printed pads in electrical designs which need to be a good electrical conduct as well as a thermal insulator.

Several more comparisons were made to analysis these dates. First, through Figure 4.1-Figure 4.8, the interfacial heat resistance is pressure dependent except for Double Sides 4 mL. With the pressure rising, all values decreased. This may because the air gap between the contact surfaces and the uneven contact interface. When the pressure went up, the surfaces contact better and the air was removed by force. Additionally, more decrease occurred when the pressure raised from 20 psi to 40 psi, comparing to the decrease occurred when the pressure rose from 40 psi to 60psi as well as that one from 60 psi to 80 psi. It could be seen very clearly from Figure 4.9 and Figure 4.10. The trends of those lines were getting smoother and smoother when the pressure increased.

Second, according to Figure 4.11 and 4.12, the trend of 8 mL line in the single side group was smoother than that of 2 mL. And the situation also occurred on the trend of 12 mL line. Comparing to the trend of 4 mL line and 8 mL line in the double sides group, the trend of 12 mL line is the smoothest. That means more CNTs were printed on the substrate, less influence with the pressure for the thermal interfacial resistance. The thermal interfacial resistance was higher with the more CNTs printed films since those CNTs are random network MWNTs which may have more thermal joints and limit the heat transfer. Also, more volume of CNT solution means more SDS was applied as surfactant which may limit the heat transport.

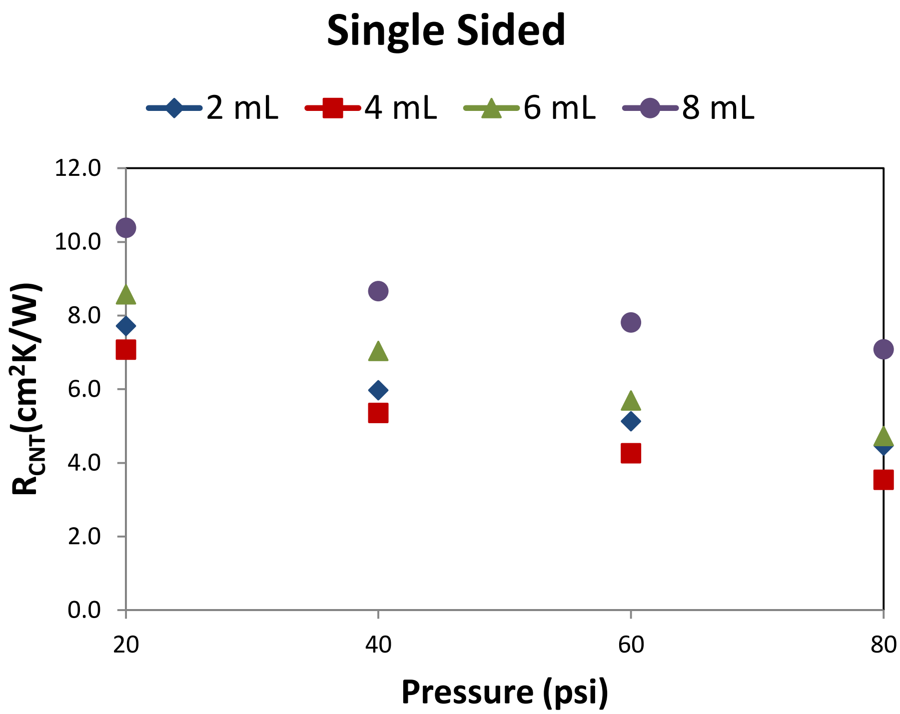

Figure 4.9 Average Thermal Resistance of Single Sided printed CNT Films

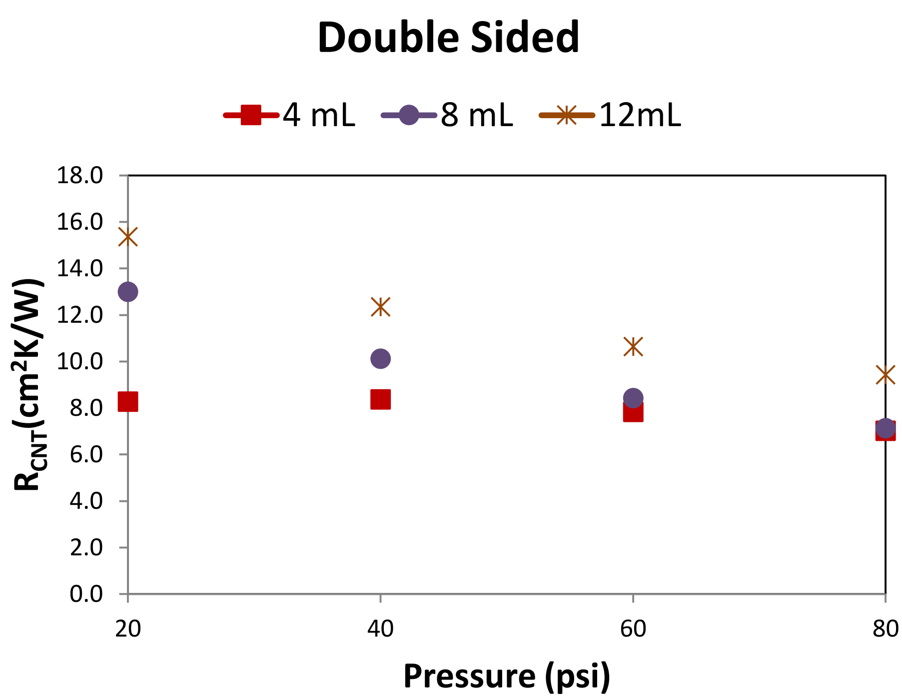

Figure 4.10 Average Thermal Resistance of Double Sided printed CNT Films

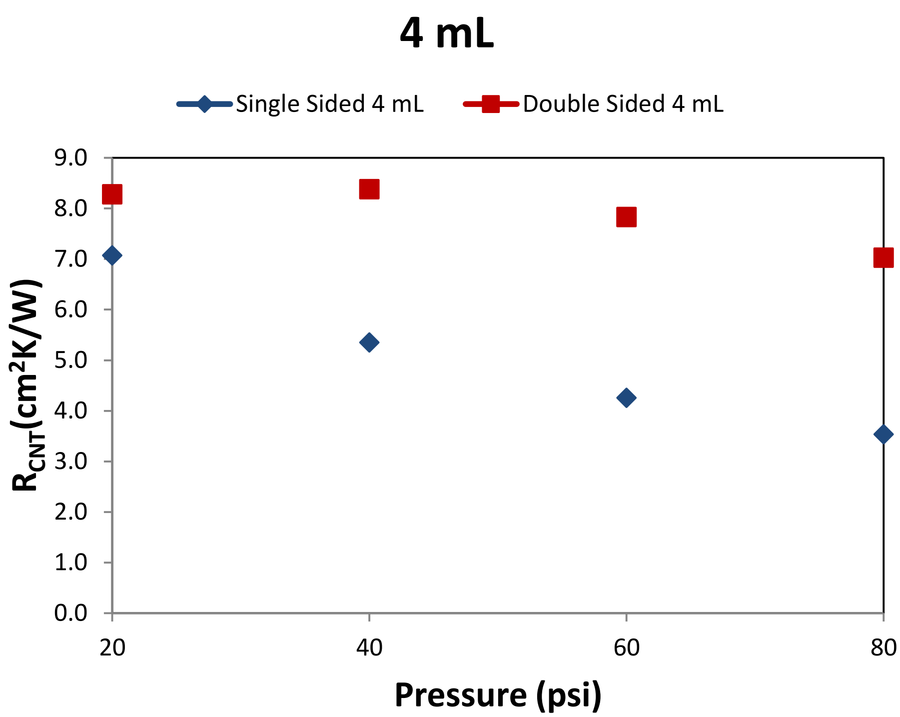

Figure 4.11 Average Thermal Resistance of 4 mL printed CNT Films

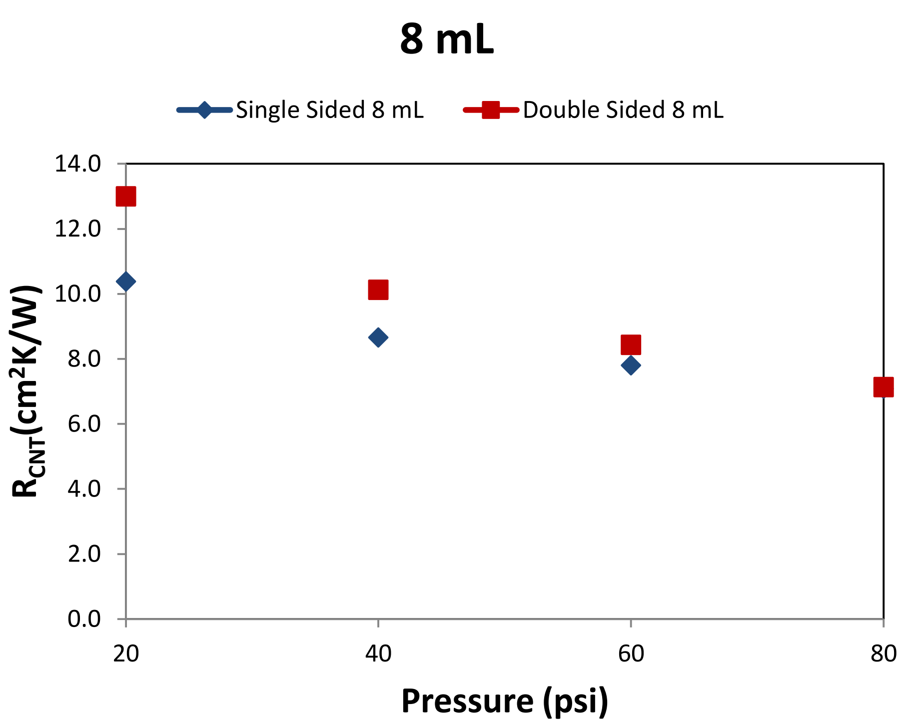

Figure 4.12 Average Thermal Resistance of 8 mL printed CNT Films

When the volume of the solution controlled to be same, the thermal interfacial resistance of double sided of the CNT solution films was higher than that of single sided, which could be seen clearly in Figure 4.9and 4.10. The difference in the heat resistance was more obvious between the 4 mL single sided and double sided set other than 8 mL single sided and double sided set.

Chapter 5

Conclusions and Recommendations

According to the experimental results obtained here, the solution deposited MWNTs-SDS films behave more like thermal insulators since the average thermal interfacial resistance of those samples ranged from 3.534cm^{2}K/W to 15.364 cm^{2}K/W which are one order of magnitude higher than that of the bare copper disk. The reasons might include some of the following respects:

1) Uneven and unsmooth contact surface of the MWNTs films. This may cause air gaps and incomplete contact area which lead high thermal transport resistance.

2) The MWNTs are uniform distribution in the films. This may cause the thermal resistance to be very high in the area where the MWNTs assembled

3) The surfactant SDS are used to disperse may have increased the thermal resistance of the film significantly

4) The random network MWNTs used to fabricate the films had the highest thermal resistance among all kinds CNTs materials due to its tube-tube junctions.

5) The measured total thermal resistance is including the resistance of the interface between the MWNT-substrate and MWNT-MWNT as well as the resistance of the film itself. In order to get an accurate thermal resistance measurement of the film, more work should be done to obtain the interface contact resistance.

The thickness of the MWNTs-SDS films could be measured in future work in order to quantify their affect. A pressure dependent modelling and simulation effort could also be conducted in order to get an accurate estimate on the thermal resistance of these films and develop the theoretical analysis of the solution-based inkjet printed MWNTs-SDS films. Additionally, the surface geometries need to be measured and inspected in order to understand the effects of surface topologies.

Reference

[1] P. Xu, F. Tong, V. A. Davis, M. Park and M. C. Hamilton, "Solution-Based Fabrication of Carbon Nanotubes Bumps fo Flip-Chip Interconnects," *IEEE Transactions on Nanotechnology,* vol. 13, no. 6, pp. 1118-1126, 2014. DOI:10.1109/TNANO.2014.2340132

[2] P. Xu and H. C. Michael, "Solution-Deposited Carbon Nanotube Flip Chip Interconnect for High-Frequency Applications," *Microwave and Wireless Components Letters,IEEE,,* vol. 25, no. 4, pp. 229-231, 2015. DOI: 10.1109/LMWC.2015.2400926

[3] S. Lijima, "Helical Microtubules of Graphitic Carbon," *Nature,* vol. 354, pp. 56-58, 1991.

[4] X. Wang, Q. Li, J. Xie, Z. Jin, J. Wang, Y. Li, K. Jiang and S. Fan, "Fabrication of Ultralong and Electrivally Uniform Single-Walled Carbon Nanotubes on Clean Substrates," *Nano Letters,* vol. 9, no. 9, pp. 3137-3141, 2009.

[5] M. Gaillard, H. Mbitsi, A. Petit, E. Amin-Chalhoub, C. Boulmer-Leborgne, N. Semmar, E. Millon, J. Mathias and S. Kouassi, "Electrical and Theraml Chatacterization of Carbon Nanotube Films," *Vacuum Science & Technology B,* vol. 29, no. 4, p. 041805, 2011.

[6] H. Park, A. Afzali, S.-J. Han, G. S. Tulevski, A. D. Franklin, J. Tersoff, J. B. Hannon and W. Haensch, "High-Density Intergration of Carbon Nanotubes via Chemical Self-Assembly," *Nature Nanotechnology,* vol. 7, pp. 787-791, 2012.

[7] S. Berber, Y.-K. Kwon and D. Tomanek, "Unusually High Thermal Conductivity of Carbon Nanotubes," *Physical Review Letters,* vol. 84, no. 20, pp. 4613-4616, 2000.

[8] J. Hone, M. C. Llaguno, M. J. Biercuk, A. T. Johnson, B. Batlogg, Z. Benes and J. E. Fischer, "Thermal Properties of Carbon Nanotubes and Nanotubes-based Materials," *Applied Physics A,* vol. 74, pp. 339-343, 2002.

[9] R. S. Prasher, X. Hu, Y. Chalopin, N. Mingo, K. Lofgreen, S. Volz, F. Cleri and P. Keblinski, "Turning Carbon Nanotuebs from Exceptional Heat Conductors into Insulators," *Physical Review Letters,* vol. 102, no. 10, p. 105901, 2009.

[10] J. Emsley, Nature's Building Blocks: an AZ Guide to the Elements, Oxford University Press, 2001.

[11] R. S. Ruoff and D. L. Lorents, "Mechanical and Thermal Properties of Carbon Nanotubes," *Carbon Nanotubes,* vol. 33, no. 7, pp. 925-930, 1995.

[12] P. Kim, L. Shi, A. Majumdar and P. McEuen, "Thernal Transport Measurement of Individual Multiwalled Nanotubes," *Physical Review Letters,* vol. 87, no. 21, p. 215502, 2001.

[13] T. Y. Choi, D. Poulikakos, J. Tharian and U. Sennhauser, "Measurement of Thermal Conductivity of Individual Multiwalled Carbon Nanotubes by the 3ω Method," *Applied Physics Letters,* vol. 87, no. 1, p. 013108, 2005.

[14] D. Yang, Q. Zhang, G. Chen, S. Yoon, J. Ahn, S. Wang, G. Zhou, Q. Wang and J. Li, "Thermal Conductivity of Multiwalled Carbon Nanotubes," *Physical Review B,* vol. 66, no. 16, p. 165440, 2002.

[15] A. E. Aliev, M. H. Lima, E. M. Silverman and R. H. Baughman, "Thermal Conducivity of Multi-Walled Carbon Nanotube Sheets: Radiation Losses and Quenching of Phonon Modes," *Nanotechnology,* vol. 21, no. 3, p. 035709, 2010.

[16] Y. Juekuan, S. Waltermire, Y. Chen, A. A. Zinn, T. T. Xu and D. Li, "Contact Thermal Resistance Between Individual Multiwall Carbon Nanotubes," *Applied Physics Letters,* vol. 96, no. 2, p. 023109, 2010.

[17] S. Sheng, E. Sichel and J. Gittleman, "Fluctuation-induced Tunneling Conduction in Carbon-polyvinylchloride Composites," *Phys. Rev. Lett.,* vol. 40, p. 1197, 1978.

[18] B.-W. Huang, T.-K. Hsiao, K.-H. Lin, D.-W. Chiou and C.-W. Chang, "Length-dependent Thermal Transport and Ballistic Thermal Conduction," *AIP Adavances,* vol. 5, p. 053202, 2015.

[19] J. Wang, L. Li and J.-S. Wang, "Tuning Thermal Transport in Nanotubes with Topological Defects," *Applied Physics Letters,* vol. 99, p. 091905, 2011.

[20] M. Hu and D. Poulikakos, "Si/Ge Superlattice Nanowires with Ultralow Thermal Conductivity," *Nano Letters,* vol. 12, pp. 5487-5494, 2012.

[21] T. Tong, Y. Zhao, L. Delzeit, A. Kashani, M. Meyyappan and A. Majumdar, "Dense Vertically Aligned Multiwalled Carbon Nanotube Arrays as Thermal Interface Materials," *IEEE Transactions on Components and Packaging Technonlgies,* vol. 30, no. 1, pp. 92-100, March 2007.

[22] B. A. Cola, "Carbon Nanotubes as High Performance Thermal Interface Materials," *ElectronicsCooling,* vol. 16, no. 1, pp. 10-15, 2010.

[23] B. A. Cola, J. Xu and T. S. Fisher, "Contact Mechanics and Thermal Conductance of Carbon Nanotube Array Interfaces," *International Journal of Heat and Mass Transfer,* vol. 52, no. 15-16, pp. 3490-3503, 2009.

[24] B. A. Cola, P. B. Amama, X. Xu and T. S. Fisher, "Effects of Growth Temperature on Carbon Nanotube Array Thermal Interfaces," *Journal of Heat Transfer,* vol. 130, no. 11, p. 114503, 2008.

[25] B. A. Cola, X. Xu and T. S. Fisher, "Increased Real Contact in Thermal Interfaces: A Carbon Nanotube/Foil Material," *Applied Physics Letters,* vol. 90, no. 9, p. 093513, 2007.

[26] B. A. Cola, J. Xu, C. Cheng, X. Xu, T. S. Fisher and H. Hu, "Photoacoustic Characterization of Carbon Nanotube Array Thermal Interfaces," *Journal of Applied Physics,* vol. 101, no. 5, p. 054313, 2007.

[27] B. A. Cola, *Photoacoustic Characterization and Optimization of Carbon Nanotube Array Thermal Interface,* West Lafayette, IN: Purdue University, 2008.

[28] P. Xu and M. C. Hamilton, "Indium Plated Carbon Nanotubes Pattern on Flexible Substrate Defined by Ink-jet Printing," *MRS Proceedings,* vol. 1505, 2013.

[29] A. R. Boccaccini, J. Cho, J. A. Roether, B. J. Thomas, E. J. Minay and M. S. Shaffer, "Electrophoretic Deposition of Carbon Nanotubes," *Carbon,* vol. 44, no. 15, pp. 3149-3160, 2006.

[30] M. Kumar and Y. Ando, "Chemical Vapor Deposition of Carbon Nanotubes: A Review on Growth Mechanism ans Mass Production," *Journal of Nanoscience and Nanotechnology,* vol. 10, no. 6, pp. 3739-3758, 2010.

[31] S. Hermann, B. Pahl, R. Ecke, S. E. Schulz and T. Gessner, "Carbon Nanotubes for Nanoscale Low Temperature Flip Chip Connections," *Microelectronic Engineering,* vol. 87, no. 3, pp. 438-442, 2010.

[32] A. S. D5470, 2012, "Standard Test Method for Thermal Transmission Properties of Thermally Conducive Electrical Insulation Materials," *ASTM International*,West Conshohocken, PA, 2012, doi: 10.1520/D5470-12, www.astm.org.

[33] K. C. Roy, S. Bhavnani, C. M. Hamilton, R. W. Johnson, J. L. Nguyen, R. W. Knight and D. K. Harris, "Investigation into the Application of Low Melting Temperature Alloys as Wet Thermal Interface Materials," *International Journal of Heat and Mass Transfer*, vol. 85, pp. 996-1002, 2015.

Appendix: All Data from Experiment

Bare

Pressure (psi)		T1(℃)	T2(℃)	ΔT(°C/K)	Q(W)	R_{CNT} (cm^2K/W)	R_{CNT} (m^2K/W)
20	1	80.207	57.568	22.639	267.4	0.642	0.0000641872
	2	80.132	58.318	21.814	274.41	0.598	0.0000597675
	3	79.021	58.488	20.533	275.66	0.555	0.0000554861
	4	79.206	59.529	19.677	282.12	0.514	0.0000514336
	5	78.569	59.824	18.745	283.15	0.484	0.0000484024
	6	78.95	60.790	18.16	288.41	0.456	0.0000456359
	7	77.55	60.560	16.99	285.79	0.426	0.0000426291
	8	78.45	61.600	16.85	291.81	0.412	0.0000411703
	9	77.31	60.980	16.33	287.09	0.404	0.0000404334
	10	77.58	61.530	16.05	289.96	0.391	0.0000391264
40	1	74.99	61.910	13.08	313.85	0.274	0.0000274329
	2	75.02	62.040	12.98	318.56	0.266	0.0000266377
	3	75.53	62.420	13.11	322.93	0.265	0.0000265105
	4	74.78	61.900	12.88	319.6	0.263	0.0000262568
	5	75.19	62.300	12.89	322.97	0.259	0.0000259238
	6	75.49	62.540	12.95	325.25	0.258	0.0000258423
	7	75.23	62.290	12.94	323.77	0.260	0.0000259715
	8	75.07	62.290	12.78	323.98	0.255	0.0000255271
	9	75.12	62.410	12.71	325.38	0.252	0.0000251980
	10	75.48	62.680	12.8	327.56	0.252	0.0000252107

Bare

Pressure (psi)		T1(℃)	T2(℃)	ΔT(°C/K)	Q(W)	R_{CNT} (cm^2K/W)	R_{CNT} (m^2K/W)
60	1	73.75	62.260	11.49	340.94	0.206	0.0000206143
	2	73.73	62.330	11.4	344.65	0.201	0.0000200809
	3	73.76	62.510	11.25	347.55	0.195	0.0000194759
	4	73.34	62.300	11.04	346.58	0.190	0.0000190353
	5	73.9	62.760	11.14	350.24	0.190	0.0000189948
	6	73.95	62.920	11.03	352.34	0.186	0.0000185658
	7	73.39	62.560	10.83	349.78	0.183	0.0000182728
	8	73.45	62.740	10.71	351.27	0.179	0.0000178684
	9	73.78	62.910	10.87	352.75	0.181	0.0000181468
	10	73.15	62.540	10.61	350.3	0.177	0.0000176965
80	1	72	62.000	10	361.03	0.155	0.0000154822
	2	72.06	62.640	9.42	365.63	0.138	0.0000138280
	3	72.51	63.020	9.49	369.89	0.137	0.0000137361
	4	72.3	62.950	9.35	370.41	0.134	0.0000133822
	5	72.2	62.950	9.25	370.71	0.131	0.0000131341
	6	72.25	63.050	9.2	372.11	0.129	0.0000129389
	7	72.14	63.020	9.12	371.72	0.128	0.0000127771
	8	71.95	62.840	9.11	370.43	0.128	0.0000128270
	9	72.19	63.050	9.14	372.41	0.128	0.0000127841
	10	72.03	63.040	8.99	373.12	0.124	0.0000124005

Single Side 2 mL

Pressure (psi)		T1(℃)	T2(℃)	ΔT(°C/K)	Q(W)	R_{CNT} (cm^2K/W)	R_{CNT} (m^2K/W)
20	1	119.042	33.301	85.741	92.95	7.805	0.000780488
	2	119.145	33.55	85.595	94.74	7.643	0.000764269
	3	119.298	33.392	85.906	94.84	7.663	0.000766258
	4	118.973	33.256	85.717	94.26	7.693	0.000769309
	5	119.538	33.123	86.415	94.14	7.766	0.00077664
	6	119.104	33.044	86.06	93.56	7.783	0.000778261
	7	119.036	33.098	85.938	93.66	7.763	0.000776308
	8	118.836	32.952	85.884	93.17	7.799	0.000779938
	9	119.661	33.201	86.46	94.43	7.746	0.000774637
	10	119.323	33.144	86.179	94.24	7.737	0.000773666
	11	119.023	33.129	85.894	94.06	7.726	0.000772572
	12	118.959	33.08	85.879	94.06	7.724	0.000772435
	13	119.121	33.124	85.997	94.25	7.719	0.000771932
	14	118.811	33.111	85.7	94.07	7.707	0.000770725
	15	118.958	33.096	85.862	94.36	7.698	0.000769799

Single Side 2 mL

Pressure (psi)		T1(℃)	T2(℃)	ΔT(°C/K)	Q(W)	R_{CNTs} (cm^2K/W)	R_{CNTs} (m^2K/W)
40	1	118.807	33.589	85.218	108.84	6.612	0.000661236
	2	117.815	33.363	84.452	109.98	6.483	0.000648342
	3	115.517	34.456	81.061	114.48	5.972	0.000597208
	4	116.932	34.74	82.192	117.3	5.909	0.000590898
	5	116.732	34.734	81.998	117.41	5.889	0.000588924
	6	117.385	34.696	82.689	117.38	5.941	0.00059411
	7	116.27	34.471	81.799	116.34	5.930	0.000592953
	8	116.357	34.518	81.839	116.64	5.917	0.0005917
	9	116.248	34.508	81.74	116.64	5.910	0.000590974
	10	116.673	34.631	82.042	115.73	5.979	0.000597917
	11	117.474	34.8	82.674	116.08	6.007	0.000600744
	12	116.22	34.55	81.67	114.75	6.003	0.000600322
	13	117.084	34.806	82.278	116.9	5.936	0.000593577
	14	116.725	34.891	81.834	116.51	5.923	0.000592333
	15	116.308	34.772	81.536	115.64	5.946	0.000594647

Single Side 2 mL

Pressure (psi)		T1(℃)	T2(℃)	ΔT(°C/K)	Q(W)	R_{CNTs} (cm^2K/W)	R_{CNTs} (m^2K/W)
60	1	116.46	35.039	81.421	125.32	5.473	0.000547298
	2	115.909	34.972	80.937	126.94	5.369	0.000536948
	3	116.283	35.181	81.102	129.01	5.293	0.000529295
	4	115.389	35.044	80.345	127.86	5.291	0.000529067
	5	116.033	35.202	80.831	130.02	5.233	0.000523337
	6	116.512	35.405	81.107	129.1	5.290	0.000528953
	7	116.217	35.532	80.685	130.71	5.196	0.000519577
	8	115.67	35.437	80.233	130.24	5.185	0.000518514
	9	115.793	35.457	80.336	131.13	5.156	0.000515611
	10	116.024	35.601	80.423	131.72	5.138	0.000513829
	11	115.525	35.483	80.042	130.74	5.153	0.00051525
	12	115.665	35.498	80.167	131.64	5.125	0.000512484
	13	115.372	35.493	79.879	131.35	5.118	0.000511758
	14	115.238	35.469	79.769	130.76	5.134	0.000513385
	15	115.86	35.626	80.234	132.22	5.106	0.000510633

Single Side 2 mL

Pressure (psi)		T1(℃)	T2(℃)	ΔT(°C/K)	Q(W)	R_{CNTs} (cm^2K/W)	R_{CNTs} (m^2K/W)
80	1	115.102	35.894	79.208	139.05	4.788	0.000478839
	2	114.462	35.871	78.591	139.88	4.722	0.000472178
	3	115.784	36.269	79.515	144.11	4.636	0.00046356
	4	115.034	36.169	78.865	143.64	4.612	0.000461235
	5	114.699	36.099	78.6	143.36	4.606	0.000460571
	6	114.568	36.127	78.441	143.97	4.576	0.00045764
	7	114.506	36.181	78.325	144.17	4.563	0.000456306
	8	115.396	36.594	78.802	145.84	4.538	0.000453784
	9	114.627	36.535	78.092	145.87	4.495	0.000449527
	10	114.704	36.387	78.317	146.56	4.487	0.000448685
	11	114.422	36.395	78.027	146.77	4.463	0.000446342
	12	115.693	36.641	79.052	148.5	4.469	0.000446948
	13	114.704	36.387	78.317	147.56	4.456	0.000445589
	14	115.353	36.982	78.371	146.33	4.497	0.000449718
	15	114.544	36.87	77.674	146.46	4.452	0.000445243

Single Side 4 mL

Pressure (psi)		T1(℃)	T2(℃)	ΔT(°C/K)	Q(W)	R_{CNTs} (cm^2K/W)	R_{CNTs} (m^2K/W)
20	1	117.356	31.920	85.436	89.5	8.080	0.000807976
	2	117.209	32.071	85.138	91.7	7.856	0.000785617
	3	116.42	32.272	84.148	92.93	7.660	0.000766001
	4	117.453	32.591	84.862	98.56	7.280	0.000727971
	5	116.486	32.722	83.764	98.7	7.174	0.000717415
	6	116.206	32.805	83.401	99.01	7.120	0.000712009
	7	115.985	32.751	83.234	99.23	7.090	0.000708973
	8	115.366	32.669	82.697	99.06	7.056	0.000705569
	9	115.985	32.637	83.348	99.72	7.064	0.000706426
	10	115.893	32.618	83.275	100.03	7.036	0.000703588
40	1	114.94	33.793	81.147	116.43	5.877	0.0005877
	2	112.536	33.643	78.893	117.24	5.671	0.000567146
	3	112.32	33.868	78.452	118.95	5.557	0.000555705
	4	115.226	34.376	80.85	123.99	5.493	0.000549319
	5	112.355	34.005	78.35	121.94	5.412	0.000541162
	6	112.311	34.061	78.25	123.14	5.351	0.000535115
	7	112.172	33.978	78.194	123.25	5.342	0.000534241
	8	113.085	34.108	78.977	125	5.320	0.000532003
	9	114.684	34.314	80.37	126.52	5.349	0.000534926
	10	113.231	34.075	79.156	123.7	5.389	0.000538917

Single Side 4 mL

Pressure (psi)		T1(℃)	T2(℃)	ΔT(°C/K)	Q(W)	R_{CNTs} (cm^2K/W)	R_{CNTs} (m^2K/W)
60	1	110.412	34.906	75.506	138.19	4.590	0.000458966
	2	110.043	35.055	74.988	140.1	4.494	0.000449436
	3	112.788	35.685	77.103	146.34	4.423	0.000442279
	4	110.364	35.249	75.115	143.47	4.394	0.000439443
	5	109.192	35.206	73.986	143.47	4.327	0.000432715
	6	112.92	35.911	77.009	149.04	4.336	0.000433579
	7	110.085	35.323	74.762	145.99	4.296	0.000429649
	8	110.048	35.517	74.531	147.49	4.239	0.000423856
	9	109.832	35.478	74.354	147.99	4.214	0.000421374
	10	110.043	35.529	74.514	148.88	4.197	0.000419725
80	1	108.699	36.100	72.599	159.02	3.821	0.000382142
	2	110.257	36.530	73.727	162.84	3.789	0.000378907
	3	108.103	36.332	71.771	162.55	3.693	0.00036931
	4	107.657	36.413	71.244	163.86	3.635	0.000363542
	5	107.977	36.556	71.421	165.74	3.602	0.000360238
	6	107.222	36.420	70.802	165.18	3.583	0.000358283
	7	109.213	36.812	72.401	168.38	3.594	0.000359438
	8	107.114	36.602	70.512	166.99	3.528	0.000352826
	9	107.483	36.792	70.691	169.26	3.489	0.000348889
	10	107.006	36.699	70.307	168.89	3.477	0.000347727

Single Side 6 mL

Pressure (psi)		T1(℃)	T2(℃)	ΔT(°C/K)	Q(W)	R_{CNTs} (cm^2K/W)	R_{CNTs} (m^2K/W)
20	1	119.966	30.797	89.169	86.04	8.779	0.000877894
	2	119.079	30.634	88.445	84.99	8.816	0.000881557
	3	119.681	30.662	89.019	85.96	8.772	0.000877226
	4	119.097	30.586	88.511	85.69	8.749	0.000874947
	5	120.229	30.623	89.606	88.33	8.592	0.000859151
	6	119.189	30.433	88.756	86.78	8.663	0.000866269
	7	119.307	30.450	88.857	87.57	8.594	0.000859366
	8	119.386	30.542	88.844	87.77	8.573	0.000857262
	9	120.251	30.615	89.636	89.55	8.476	0.000847621
	10	120.32	30.627	89.693	88.92	8.542	0.000854233
40	1	119.181	31.056	88.125	100.66	7.403	0.000740328
	2	119.585	31.143	88.442	103.78	7.204	0.000720437
	3	118.626	31.027	87.599	103.22	7.174	0.000717407
	4	119.076	31.187	87.889	104.38	7.117	0.000711719
	5	118.704	31.249	87.455	104.3	7.087	0.000708713
	6	118.815	31.252	87.563	104.69	7.069	0.000706924
	7	118.862	31.309	87.553	105.09	7.041	0.000704121
	8	118.078	31.147	86.931	104.33	7.042	0.000704213
	9	118.017	31.121	86.896	104.63	7.019	0.000701884
	10	117.991	31.072	86.919	104.73	7.014	0.000701394

Single Side 6 mL

Pressure (psi)		T1(℃)	T2(℃)	ΔT(°C/K)	Q(W)	R_{CNTs} (cm^2K/W)	R_{CNTs} (m^2K/W)
60	1	119.188	32.088	87.1	117.56	6.253	0.000625268
	2	117.304	32.013	85.291	118.06	6.095	0.000609484
	3	118.394	32.276	86.118	122.49	5.929	0.000592918
	4	117.373	32.401	84.972	122.44	5.852	0.000585161
	5	116.977	32.369	84.608	122.76	5.811	0.000581079
	6	118.631	32.610	86.021	125.88	5.761	0.00057607
	7	116.571	32.307	84.264	124.38	5.710	0.000571039
	8	115.807	32.405	83.402	123.92	5.672	0.000567241
	9	116.227	32.430	83.797	124.9	5.654	0.00056543
	10	116.168	32.333	83.835	125.2	5.643	0.000564315
80	1	116.14	33.271	82.869	137.98	5.053	0.000505302
	2	115.331	33.343	81.988	138.62	4.975	0.000497497
	3	114.87	33.264	81.606	139.44	4.922	0.000492181
	4	114.609	33.364	81.245	140.35	4.867	0.000486737
	5	114.852	33.411	81.441	141.73	4.831	0.000483101
	6	117.148	33.787	83.361	146.22	4.792	0.000479241
	7	115.486	33.605	81.881	144.7	4.756	0.000475617
	8	114.684	33.539	81.145	144.24	4.728	0.000472797
	9	114.852	33.588	81.264	145.33	4.699	0.000469889
	10	114.155	33.595	80.56	144.76	4.676	0.000467614

Single Side 8 mL

Pressure (psi)		T1(℃)	T2(℃)	ΔT(°C/K)	Q(W)	R_{CNTs} (cm^2K/W)	R_{CNTs} (m^2K/W)
20	1	117.730	31.16	86.570	70.5	10.417	0.0010416915
	2	116.910	30.67	86.240	69.86	10.473	0.0010472709
	3	116.930	30.57	86.360	69.96	10.472	0.0010472288
	4	116.940	30.55	86.390	70.16	10.446	0.0010445858
	5	117.270	30.55	86.720	70.54	10.429	0.0010429143
	6	116.780	30.57	86.210	70.17	10.422	0.0010422425
	7	117.200	30.71	86.490	70.75	10.370	0.0010370148
	8	116.810	30.67	86.140	70.47	10.369	0.0010369213
	9	116.840	30.52	86.320	70.56	10.378	0.0010377694
	10	116.930	30.55	86.380	70.76	10.355	0.0010355380
40	1	117	32.130	84.87	79.77	9.015	0.0009014634
	2	116.41	31.750	84.66	80.01	8.965	0.0008964907
	3	116.75	31.820	84.93	80.79	8.906	0.0008906136
	4	116.38	31.890	84.49	81.01	8.835	0.0008835288
	5	116.75	31.860	84.89	82.09	8.760	0.0008759631
	6	116.32	31.820	84.5	82.01	8.728	0.0008727596
	7	116.45	31.840	84.61	82.6	8.676	0.0008676057
	8	116.23	31.830	84.4	82.51	8.664	0.0008663849
	9	116.39	31.920	84.47	82.9	8.630	0.0008629924
	10	116.4	31.900	84.5	83.1	8.612	0.0008612043

Single Side 8 mL

Pressure (psi)		T1(℃)	T2(℃)	ΔT(°C/K)	Q(W)	R_{CNTs} (cm^2K/W)	R_{CNTs} (m^2K/W)
60	1	116.84	31.820	85.02	91.08	7.899	0.0007899126
	2	116.22	31.580	84.64	90.62	7.904	0.0007903787
	3	116.46	31.560	84.9	91.01	7.894	0.0007893992
	4	116.09	31.320	84.77	90.93	7.889	0.0007888785
	5	115.9	31.440	84.46	90.94	7.859	0.0007858763
	6	116.5	31.600	84.9	91.91	7.816	0.0007815889
	7	116.1	31.410	84.69	91.53	7.829	0.0007829062
	8	115.99	31.320	84.67	91.64	7.818	0.0007817700
	9	116.56	31.570	84.99	92.41	7.781	0.0007781483
	10	116.99	31.620	85.37	92.69	7.793	0.0007792782
80	1	116.09	31.690	84.4	98.45	7.248	0.0007247812
	2	116.67	31.780	84.89	99.52	7.211	0.0007211102
	3	116.28	31.840	84.44	99.34	7.186	0.0007185586
	4	116.65	31.890	84.76	100.02	7.164	0.0007163531
	5	115.49	31.560	83.93	99.18	7.153	0.0007153345
	6	116.36	31.760	84.6	100.34	7.127	0.0007126790
	7	117.03	31.800	85.23	101.5	7.097	0.0007097473
	8	115.57	31.800	83.77	100.18	7.067	0.0007067466
	9	116.47	31.840	84.63	101.33	7.059	0.0007058891
	10	116.22	31.710	84.51	101.24	7.055	0.0007055105

Double Sides 4 mL

Pressure (psi)		T1(℃)	T2(℃)	ΔT(°C/K)	Q(W)	R_{CNTs} (cm^2K/W)	R_{CNTs} (m^2K/W)
20	1	116.157	30.29	85.867	92.31	7.871	0.000787123
	2	118.019	30.08	87.941	94.12	7.907	0.000790669
	3	117.502	29.81	87.692	93.05	7.976	0.000797567
	4	118.617	29.86	88.76	93.9	8.000	0.000799998
	5	117.546	29.86	87.691	92.46	8.027	0.0008027
	6	118.651	29.65	89.003	93.1	8.092	0.000809174
	7	120.013	29.76	90.256	92.94	8.221	0.000822109
	8	118.975	29.56	89.418	91.1	8.310	0.000831014
	9	119.953	29.42	90.529	92.05	8.327	0.000832672
	10	120.149	29.38	90.771	90.95	8.451	0.000845117
40	1	119.742	29.79	89.953	98.97	7.689	0.000768902
	2	118.693	29.9	88.79	98.92	7.592	0.000759243
	3	121.11	29.84	91.267	100.9	7.652	0.000765172
	4	119.882	29.59	90.294	98.67	7.742	0.00077422
	5	120.286	29.8	90.491	99.05	7.729	0.000772919
	6	120.65	29.27	91.385	93.85	8.243	0.000824343
	7	120.198	29.07	91.126	93.08	8.289	0.000828851
	8	120.025	29.1	90.927	91.99	8.369	0.00083692
	9	120.317	28.93	91.386	91.88	8.422	0.000842203
	10	120.673	28.94	91.738	90.57	8.578	0.000857826

Double Sides 4 mL

Pressure (psi)		T1(℃)	T2(℃)	ΔT(°C/K)	Q(W)	R_{CNTs} (cm^2K/W)	R_{CNTs} (m^2K/W)
60	1	119.937	29.28	90.657	97.39	7.877	0.00078769
	2	120.342	29.42	90.92	99.77	7.710	0.000770958
	3	120.578	29.43	91.146	101.05	7.630	0.000763001
	4	120.229	29.41	90.82	100.17	7.670	0.000766993
	5	119.298	29.4	89.895	98.83	7.695	0.000769501
	6	121.453	29.34	92.109	99.53	7.831	0.000783051
	7	121.042	29.4	91.641	100.24	7.735	0.000773455
	8	120.604	29.32	91.286	100.27	7.702	0.000770194
	9	119.969	29.26	90.712	98.8	7.768	0.000776808
	10	121.187	28.95	92.238	96.06	8.128	0.000812782
80	1	119.677	29.46	90.213	102.41	7.450	0.00074497
	2	119.521	29.56	89.96	104.02	7.312	0.000731233
	3	120.459	29.84	90.617	108.27	7.074	0.000707396
	4	120.22	29.85	90.368	107.78	7.087	0.000708674
	5	119.53	29.77	89.764	107.22	7.076	0.000707601
	6	119.153	29.77	89.384	107.14	7.051	0.000705103
	7	119.752	29.86	89.888	107.8	7.047	0.000704734
	8	119.488	29.75	89.737	107.72	7.041	0.000704065
	9	120.494	30.01	90.483	109.17	7.004	0.000700447
	10	120.069	29.96	90.108	108.89	6.993	0.000699324

Double Sides 8 mL

Pressure (psi)		T1(℃)	T2(℃)	ΔT(°C/K)	Q(W)	R_{CNTs} (cm^2K/W)	R_{CNTs} (m^2K/W)
20	1	122.931	25.31	97.619	66.03	12.558	0.001255835
	2	122.857	24.94	97.913	64.75	12.847	0.001284705
	3	122.806	24.89	97.913	64.05	12.988	0.001298835
	4	123.292	24.79	98.506	63.14	13.257	0.001325703
	5	122.617	24.65	97.965	63.17	13.177	0.001317747
	6	122.894	24.59	98.3	63.35	13.185	0.001318501
	7	122.44	24.95	97.49	63.28	13.090	0.001309024
	8	123.114	24.83	98.281	64.55	12.936	0.001293586
	9	122.517	24.67	97.85	64.47	12.895	0.001289485
	10	122.439	24.74	97.697	64.48	12.873	0.001287255
40	1	123.481	24.95	98.532	76.32	10.956	0.001095637
	2	122.174	25	97.175	76.49	10.780	0.001078016
	3	122.494	24.96	97.535	77.56	10.670	0.001066999
	4	123.019	24.98	98.041	78.64	10.577	0.001057734
	5	122.861	24.97	97.889	79.45	10.452	0.001045231
	6	122.479	25.05	97.434	80.66	10.246	0.001024605
	7	122.334	25.44	96.894	81.07	10.137	0.001013687
	8	122.445	25.24	97.202	81.56	10.108	0.001010776
	9	122.065	25.07	96.992	81.48	10.096	0.001009573
	10	122.131	25.5	96.631	81.78	10.021	0.001002065

Double Sides 8 mL

Pressure (psi)		T1(℃)	T2(℃)	ΔT(°C/K)	Q(W)	R_{CNTs} (cm^2K/W)	R_{CNTs} (m^2K/W)
60	1	121.456	25.55	95.904	89.51	9.079	0.000907876
	2	122.45	25.85	96.6	93.26	8.774	0.000877421
	3	122.125	25.93	96.2	93.87	8.680	0.000868022
	4	122.162	26.05	96.116	93.82	8.677	0.000867724
	5	122.534	26.01	96.523	94.6	8.642	0.00086418
	6	121.189	26.1	95.089	94.71	8.502	0.000850221
	7	121.965	26.01	95.955	95.97	8.467	0.000846666
	8	121.45	25.85	95.6	95.92	8.439	0.000843948
	9	120.99	26.12	94.867	95.82	8.383	0.000838296
	10	121.203	26.04	95.162	96.41	8.357	0.000835732
80	1	121.999	26.68	95.317	105.49	7.643	0.000764347
	2	122.584	26.89	95.692	108.86	7.434	0.000743377
	3	120.386	26.89	93.499	107.34	7.366	0.000736552
	4	120.328	27	93.333	108.94	7.243	0.000724311
	5	121.561	27.1	94.458	110.78	7.208	0.000720827
	6	120.408	26.9	93.504	109.94	7.190	0.000718978
	7	120.452	26.95	93.501	110.83	7.131	0.000713115
	8	120.166	26.88	93.284	110.24	7.153	0.000715293
	9	120.428	26.94	93.49	111.13	7.111	0.000711083
	10	120.463	27.14	93.326	111.13	7.098	0.000709822

Double Sides 12 mL

Pressure (psi)		T1(℃)	T2(℃)	ΔT(°C/K)	Q(W)	R_{CNTs} (cm^2K/W)	R_{CNTs} (m^2K/W)
20	1	120.798	30.665	90.133	49.9	15.362	0.001536163
	2	120.574	30.253	90.321	49.82	15.419	0.001541869
	3	120.915	30.146	90.769	49.91	15.467	0.001546749
	4	120.742	30.129	90.613	49.81	15.472	0.001547193
	5	119.429	29.936	89.493	49.08	15.508	0.001550816
	6	120.926	30.249	90.677	50.51	15.267	0.001526721
	7	121.126	29.889	91.237	50.51	15.362	0.0015362
	8	121.157	29.969	91.188	50.41	15.384	0.001538432
	9	120.48	29.75	90.73	49.93	15.455	0.001545458
	10	121.464	29.972	91.492	50.69	15.350	0.001535017
40	1	119.578	30.528	89.05	58.77	12.873	0.001287321
	2	119.594	30.811	88.783	59.57	12.661	0.00126609
	3	119.802	30.992	88.81	60.15	12.542	0.001254187
	4	120.967	30.853	90.114	61.2	12.507	0.001250746
	5	119.252	30.634	88.618	60.29	12.485	0.001248532
	6	119.619	30.613	89.006	60.87	12.420	0.001242007
	7	119.595	30.651	88.944	60.97	12.391	0.001239088
	8	119.258	30.651	88.607	60.89	12.360	0.001235994
	9	119.706	30.675	89.031	61.56	12.283	0.001228342
	10	119.657	30.779	88.878	61.17	12.341	0.001234087

Double Sides 12 mL

Pressure (psi)		T1(℃)	T2(℃)	ΔT(°C/K)	Q(W)	R_{CNTs} (cm^2K/W)	R_{CNTs} (m^2K/W)
60	1	120.353	31.198	89.155	69.33	10.913	0.001091288
	2	118.741	31.003	87.738	68.91	10.804	0.001080408
	3	118.233	30.885	87.348	68.83	10.768	0.001076829
	4	118.789	31.101	87.688	69.41	10.720	0.00107195
	5	120.495	31.012	89.483	70.82	10.721	0.001072116
	6	118.4	30.704	87.696	69.13	10.764	0.001076424
	7	119.253	31.143	88.11	70.39	10.620	0.001062038
	8	119.073	30.784	88.289	70.3	10.656	0.001065585
	9	119.335	30.84	88.495	70.78	10.608	0.001060792
	10	120.377	31.221	89.156	71.33	10.605	0.001060472
80	1	118.373	31.281	87.092	75.62	9.765	0.000976509
	2	118.629	31.258	87.371	76.8	9.645	0.000964485
	3	119.696	31.331	88.365	77.95	9.610	0.000961038
	4	117.827	31.287	86.54	76.35	9.609	0.000960912
	5	119.669	31.209	88.46	78.56	9.545	0.000954546
	6	117.852	31.128	86.724	77.74	9.456	0.000945608
	7	118.947	31.158	87.789	78.79	9.445	0.000944454
	8	118.077	31.028	87.049	78.03	9.456	0.000945624
	9	118.499	31.307	87.192	78.81	9.377	0.000937735
	10	118.691	31.191	87.5	78.9	9.400	0.000939994